EGE UNIVERSITY GRADUATE SCHOOL OF NATURAL AND APPLIED SCIENCES

(MASTER OF SCIENCE THESIS)

PHOTOPYHSICAL AND COMPUTATIONAL INVESTIGATION OF INTERACTIONS BETWEEN SOME POLYAROMATIC HYDROCARBONS AND PORPHYRINS

Zeliha Gamze ALP

Thesis Advisor: Assist. Prof. Dr. Nursel ACAR SELÇUKİ

Department of Chemistry

Department Code :405.04.01
Presentation Date :13.06.2011

Bornova-İZMİR
2011

Zeliha Gamze ALP tarafından yüksek lisans tezi olarak sunulan "Photopyhsical and computational investigation of interactions between some polyaromatic hydrocarbons and porphyrins" başlıklı bu çalışma E.Ü. Lisansüstü Eğitim ve Öğretim Yönetmeliği ile E.Ü. Fen Bilimleri Enstitüsü Eğitim ve Öğretim Yönergesi'nin ilgili hükümleri uyarınca tarafımızdan değerlendirilerek savunmaya değer bulunmuş ve .....tarihinde yapılan tez savunma sınavında aday oybirliği/oyçokluğu ile başarılı bulunmuştur.

Jüri Üyeleri: **İmza**

Jüri Başkanı: Yrd.Doç.Dr.Nursel ACAR SELCUKİ **…….**

Üye : Doç.Dr. Armağan KINAL **……**

Üye : Doç.Dr.Cenk SELÇUKİ **……**

ÖZET

BAZI POLİAROMATİK HİDROKARBONLAR VE PORFİRİNLER ARASINDAKİ ETKİLEŞİMLERİN FOTOFİZİKSEL VE HESAPSAL YÖNTEMLERLE İNCELENMESİ

ALP, Gamze Zeliha

Yüksek Lisans Tezi, Kimya Bölümü
Tez Danışmanı: Yrd. Doç. Dr. Nursel ACAR SELÇUKİ
Haziran 2011, 72 sayfa

Bu tezde, donör-akseptör molekülleri arasında oluşan yük transfer kompleksleri fotofiziksel ve hesapsal yöntemler kullanılarak incelenmiştir. Pren ve 1-Hidroksipren akseptör olarak seçilirken, protoporphyrin (IX) donör olarak kullanılmıştır. Deneysel kısımda donör-akseptör komplekslerinin UV-Vis absorpsiyon ve fluoresans spektrumları, orta polariteye sahip çözücülerde incelenmiştir. Spektrofotometrik sonuçlara göre, akseptör moleküllerinin monomer fluoresans şiddetlerinde donör ilavesiyle sönüm olduğu gözlenmiştir ve exciplex oluşumuna ilişkin hız sabitleri 10^{10} $M^{-1}s^{-1}$ olarak difüzyon kontrollü hız sabiti mertebesinde hesaplanmıştır.

Bu çalışmanın hesapsal kısmında, DFT-PBE1PBE fonksiyonları ile temel hal geometrileri elde edilmiştir. Bu moleküllerin temel hal geometrileri, aynı teori seviyesinde harmonik titreşim frekans analizi hesaplarıyla karakterize edilmiştir. Ayrıca,TD-DFT-B3LYP fonksiyonları ile elektronik geçişlere ait uyarılma enerjileri hesaplanmışveTD-DFT-B3LYP yöntemiyle elde edilen molekül orbital yapıları ile bu geçişler karakterize edilmiştir.

Anahtar Sözcükler: Aromatik hidrokarbonlar, exciplex, moleküller arası yük transferi, fluoresans sönüm.

ABSTRACT

PHOTOPHYSICAL AND COMPUTATIONAL INVESTIGATION OF INTERACTIONS BETWEEN SOME POLYAROMATIC HYDROCARBONS AND PORPHYRINS

ALP, Gamze Zeliha

MSc in Department of Chemistry
Supervisor: Assist. Prof. Dr. Nursel ACAR SELÇUKİ
Haziran 2011, 72 pages

In this thesis, donor-acceptor intermolecular charge transfer complexes have been investigated by using photopyhsical and computational methods. Pyrene and 1-Hydroxypyrene have been selected as acceptors while protoporphyrin (IX) has been selected as donor. In experimental part, UV-Vis absorption and fluorescence spectra of donor-acceptor complexes have been recorded in several solvents with different polarity. According to spectrophotometric results, it is observed that the monomer fluorescence intensity which belongs to the acceptors is quenched by addition of the donor. This quenching is explained by the exciplex formation between donor-acceptor molecules and the rate constant for exciplex formation have been determined as the diffusion controlled rate constants in the order of and $10^{10}M^{-1}s^{-1}$.

In computational part, the ground state geometries obtained from DFT-PBE1PBE functional. These ground state geometries are characterized by the harmonic vibrational frequencies at the same level of theory. Furthermore, excitation energies of the electronic transitions have been calculated by TD-DFT-B3LYP method and these transitions were characterized with molecular orbitals obtained from TD-DFT-B3LYP calculations.

Keywords: Aromatic hydrocarbons, exciplex, intermolecular charge transfer, quenching.

ACKNOWLEDGEMENTS

I would like to thank my advisor Assist. Prof. Dr. Nursel Acar Selçuki for her help and sharing her precious knowledge during my graduate studies. I would like also like to thank Assoc. Prof. Dr. Armağan Kınal for his help with Computational Chemistry.
For provided facilities I would like to thank the department members at the Department of Chemistry; particularly to members of the physical chemistry division for support during my work.
I would like to thank also my close friend for their friendship, and also I wish to thank my friend Sinan Sayhan for support in my studies.
And I would like to thank my family for their moral support every time.

TABLE OF CONTENTS

TABLE OF CONTENTS(CONTINUE)

Page

TABLE OF CONTENTS(CONTINUE)

Page

TABLE OF CONTENTS(CONTINUE)

Page

LIST OF FIGURES

Figure Page

LIST OF FIGURES(CONTINUE)

Figure Page

LIST OF FIGURES(CONTINUE)

Figure Page

LIST OF FIGURES(CONTINUE)

Figure Page

LIST OF TABLES

LIST OF TABLES(CONTINUE)

Table Page

LIST OF SYMBOLS

Symbols	Description
E	Energy
h	Planck constant
ν	Frequency
S_0, S_1 , S_2	Singlet electronic states
T_1, T_2	Triplet electronic states
V	Vibrational levels
F	Final state
ν□	Wave number
ΔE	The energy gap
ΔE_{ST}	Singlet-triplet energy gap
N_0	Initial population k_f is the, and is
k_f	Emmisive rate
k_d	The rate of nonradiative decay
k_{ISC}	The rate coefficient for intersystem crossing
k_{IC}	The rate coefficient for internal conversion

M*, A*	Excited state of a molecule
k_q	The rate constant for exciplex formation
Ψ	Wave function
A	Electron acceptor
D	Electron donor
Q	Quencher
μ	Dipole moment
α	Average polarizability
D	Dielectric constant
K_{SV}	Stern-Volmer constant
τ_0	Life time
[Q]	Concentration of quencher
[F]	Concentration of uncomplexed fluorophore

Abbreviation

PAH	Poliaromatic hydrocarbons
Py	Pyrene
PyOH	Hydroxyprene
Porp	Porphyrin
Protoporp	Protoporphyrin

DCM	Dichloromethane
THF	Tetrahydrofuran

Abbreviations

CT	Charge Transfer
CRIP	Contact radical ion pair
SSRIP	Solvent seperated radical ion pair
MM	Molecular mechanics
DFT	Density functional theory

1. INTRODUCTION

Polycyclic aromatic hydrocarbons (**PAH**s), also known as **polyaromatic hydrocarbons** or **polynuclear aromatic hydrocarbons** are potent atmospheric pollutants that consist of fused aromatic ring and do not contain heteroatoms or carry substituents (Fetzer, 2000). PAHs are one of the most widespread organic pollutants. In addition to their presence in fossil fuels they are also formed by incomplete combustion of carbon-containing fuels such as wood, coal, diesel, fat, tobacco, and incense.

Porphyrins are a group of organic compounds of which many occur in nature. Porphyrins are heterocyclic macrocycles composed of four modified pyrrole subunits interconnected at their α-carbon atoms via methine bridges (=CH-). Porphyrins are also aromatic molecules highly-conjugated systems. As a consequence, they typically have very intense absorption bands in the visible region and may be deeply colored; the name **porphyrin** comes from a Greek word for *purple*. The macrocycle has 26 pi electrons in total. The parent porphyrin is porphine, and substituted porphines are called porphyrins. Porphyrins optoelectronics, coordination, redox, and biological/medical facilities such as the show many important and rare features. The nitrogen atoms of pyrols in the porphyrin ring system can form chelate with iron, magnesium, copper, zinc. Porphyrins can also be used as metal-porphyrins. Photophysical properties by selecting a suitable metal porphyrins, by increasing the number of pyrrole units (expanded porphyrins), or sometimes can be adjusted by adding long branches (Shinoda, 2007).

The investigation of proton donor-acceptor and electron donor-acceptor systems of aromatic compounds were first performed by Förster in 1950 explaining the reaction of aromatic hydroxyl compound which progress on the protolic reactions in water. Förster and Kasper, in 1955, first showed that pyrene forms fluorescent excited dimers or excimers in solution. The lifetime measurements of dimer and excimer of pyrene and its dependence on solvent

viscosity and temperature were investigated by many authors (Birks et al., 1964, Mataga et al., 1956, Birks et al., 1971).

1.1 Photochemical and Photopyhsical Processes

Photochemistry is the study of the chemical reactions and physical changes that result from interactions between matter and visible or ultraviolet light. The development of the quantum theory in the early twentieth century allowed predictions to be made relating to the properties and behavior of matter and light. The electrons in matter have both wavelike and particle – like properties and quantum theory shows that the energy of matter is quantized; that is, only certain specific energies are allowed. The quantized energy levels of matter have a separation that is of the same order as the energy of visible or ultraviolet light. Thus the absorption of visible or ultraviolet light by matter can excite electrons to higher energy levels, producing electronically-excited species (Wardle, 2009).

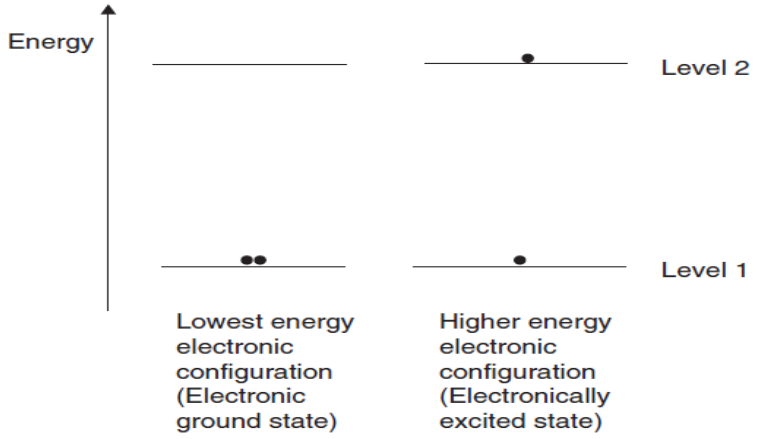

Figure 1.1 Quantized energy levels in matter, where an electron (●) may be found in either of the two energy levels shown

According to the quantum theory, light is also quantized. The absorption or emission of light occurs by the transfer of energy as photons. These photons have both wavelike and particle - like properties and each photon has a specific energy, E, given by Planck's law:

$$E=h.\nu \qquad (1.1)$$

where h is Planck's constant (6.63×10^{-34} Js) and ν is the frequency of oscillation of the photon in units of s^{-1} or Hertz (Hz) (Wardle, 2009).

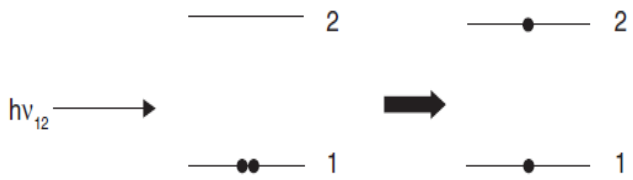

Figure 1.2 The process of light absorption.

Sometimes electronic excitation can result in chemical changes, such as the fading of dyes, photosynthesis in plants, suntans, or even degradation of molecules. On other occasions, the electronically - excited state may undergo deactivation by a number of physical processes, either resulting in emission of light (luminescence) or conversion of the excess energy into heat, whereby the original ground state is reformed. Electronically - excited states can also interact with ground-state molecules, resulting in energy-transfer or electron-transfer reactions provided certain criteria are met. There are three basic processes of light– matter interaction (a, b, c) that can induce transfer of an electron between two quantized energy states:

a. **In absorption** of light, a photon having energy equal to the energy difference between two electronic states can use its energy to move an electron from the lower energy level to the upper one, producing an electronically-excited state (Figure 1.2). The photon is completely destroyed in the process, its energy becoming part of the total energy of the absorbing species.

Two fundamental principles relating to light absorption are the basis for understanding photochemical transformations:

- The Grotthuss–Draper law states that only light which is absorbed by a chemical entity can bring about photochemical change.

- The Stark–Einstein law states that the primary act of light absorption by a molecule is a one-quantum process. That is, for each photon absorbed only one molecule is excited. This law is obeyed in the vast majority of cases but exceptions occur when very intense light sources such as lasers are used for irradiation of a sample. In these cases, concurrent or sequential absorption of two or more photons may occur.

b. **Spontaneous emission** occurs when an excited atom or molecule emits a photon of energy equal to the energy difference between the two states without the influence of other atoms or molecules.

$$R^* \longrightarrow R + h\nu_{12}$$

Light is emitted from the bulk material at random times and in all directions, such that the photons emitted are out of phase with each other in both time and space. Light produced by spontaneous emission is therefore called incoherent light.

c. **Stimulated emission** occurs when a photon of energy equal to the energy difference between the two states interacts with an excited atom or molecule.

$$R^* + h\nu_{12} \longrightarrow R + 2h\nu_{12}$$

The photons produced by stimulated emission are in phase with the stimulating photons and travel in the same direction; that is, the light produced by stimulated emission is coherent light. Stimulated emission forms the basis of laser action (Wardle, 2009).

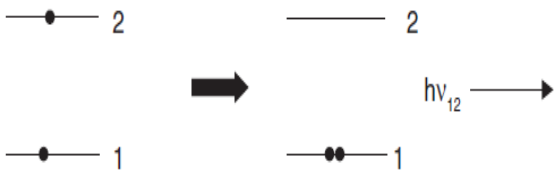

Figure 1.3 The process of spontaneous emission

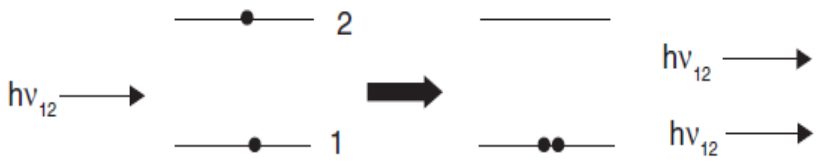

Figure 1.4 The process of stimulated emission

1.2 Interactions Between Light and Matter

1.2.1 Jablonski Diagram

The properties of excited states and their relaxation processes are conveniently represented by a Jablonski diagram, shown in Figure 1.5.

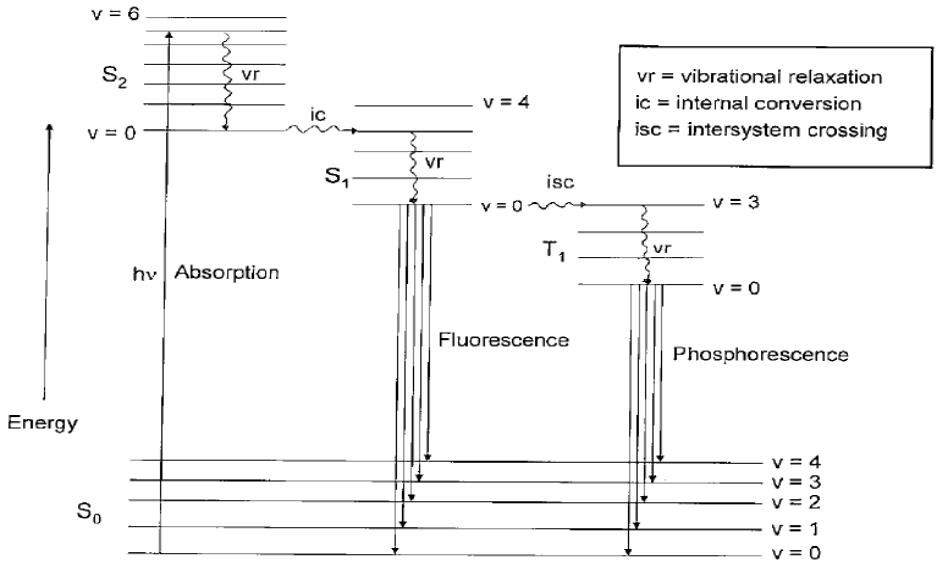

Figure 1.5 Jablonski diagram for an organic molecule, illustrating excited–state photophysical processes

The Jablonski diagram shows:

- The electronic states of the molecule and their relative energies. Singlet electronic states are denoted by S_0, S_1, S_2, etc. and triplet electronic states as T_1, T_2, etc.

- Vibrational levels associated with each state are denoted as v = 0, v = 1, v = 2, etc. in order of increasing energy.
- Radiative transitions are drawn as straight arrows and radiationless transitions as wavy arrows.
- If an electronically excited state is formed as a 'vibrationally hot' excited molecule (with v > 0) then it will undergo vibrational relaxation within that electronic energy level until it reaches then v = 0 level. The vibrational relaxation within each electronically-excited state is drawn as a vertical wavy arrow.
- Radiationless transitions (internal conversion and intersystem crossing) between electronic states are isoenergetic processes and are drawn as wavy arrows from the v = 0 level of the initial state to a 'vibrationally - hot' (v > 0) level of the final state.

1.2.2 Electronic Absorption and Emission

In absorption and emission spectra, light intensity is plotted as a function of one of the characteristics that identify photon energy. The relation $E = h\nu$ provides a bridge from the position of the observed spectral peaks to the energy difference between initial (G) and final (F) state involved in a spectroscopic transition.

The vast majority of transitions are being studied under conditions in which a single photon is absorbed by a molecule at a time, and the resonant condition for absorption or emission then is that hν be equal to the energy difference of final and initial state. Simultaneous absorption of two and at times an even larger number of photons is also possible with high laser light intensities. In two-photon absorption, if both photons are taken from the same beam, the resonance condition is that 2hν be equal to the energy difference of final and initial, etc. Some of the advantages of two photon absorption are a different set of selection rules, higher spatial resolution, and deeper penetration of the longer-wavelength exciting light into otherwise poorly transparent samples, such as biological tissue.

At room temperature equilibrium, organic molecules normally are in their electronic ground state S_0, and measurement of an absorption spectrum provides

information about transitions from S_0 to electronically excited states. It is also possible to transfer a large fraction of molecules to an excited state, typically S_1 or T_1, usually with an intense laser pulse, and to measure the absorption spectrum of this excited state. Since the excited state population decays rapidly unless continually replenished, this is referred to as transient absorption spectroscopy.

Ordinary (one-photon) absorption spectroscopy relies on the Lambert-Beer law, which relates the intensity I($\tilde{\nu}$) of monochromatic light of wave number $\tilde{\nu}$ transmitted through a sample to the intensity I_0($\tilde{\nu}$) incident on the sample:

$$I = I_0 e^{-\sigma(\tilde{\nu})l} = I_0 10^{-\varepsilon(\tilde{\nu})cl} \tag{1.2}$$

where σ($\tilde{\nu}$) is the absorption coefficient of the sample and l is its thickness. For solutions, it is common to use the molar decadic absorption coefficient (molar absorptivity) ε($\tilde{\nu}$), obtained from the above expression by inserting the molar concentration c and the sample thickness in cm.

In order to observe emission spectra of organic molecules, their excited electronic states first need to be populated. When this is done by light absorption, the emission is referred to as photoluminescence. The measurement can be performed in a continuous mode of excitation (steady state photoluminescence) or with pulsed excitation (pulsed photoluminescence). Since both the wavelength of the exciting light and that of the detected emitted light can be varied, photoluminescence is intrinsically a two-dimensional spectroscopic technique, but the full two dimensional spectra are rarely measured. A spectrum showing the dependence on the frequency (or wavelength) of the emitted light is referred to as an emission spectrum, and a spectrum showing the dependence on the frequency (or wavelength) of the exciting light of constant intensity is called the excitation spectrum.

In the absence of heavy atoms in the molecule, transitions interconnecting S and T states have small transition moments and are referred to as spin-forbidden.

In absorption, singlet-triplet (and triplet-singlet) transitions have very small extinction coefficients, and are very difficult to observe. Such singlet-triplet

absorption spectra consist of three spectrally nearly identical essentially unresolvable contributions, usually of widely different intensities, one into each of the triplet sublevels. In emission, such transitions have very small radiative constants and very long natural radiative lifetimes, and often have low quantum yields since competing radiationless processes can readily prevail. The resulting emission is referred to as phosphorescence, whereas spin-allowed emission is referred to as fluorescence (Tylor, 2006).

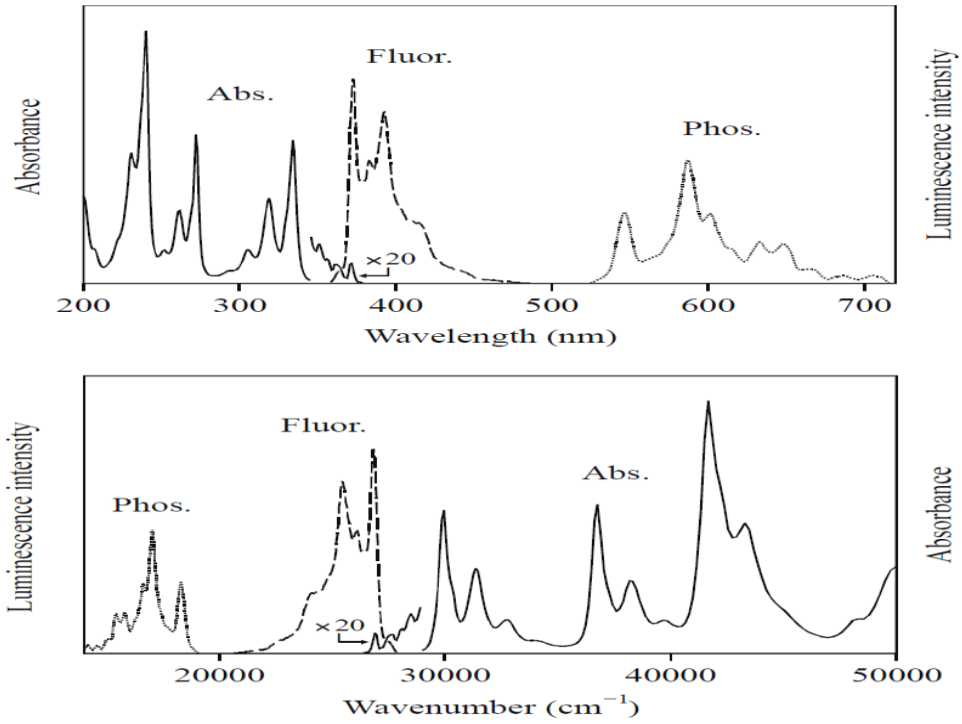

Figure 1.6 Absorption and emission spectra of pyrene. Absorption and fluorescence spectra recorded in acetonitrile solution at room temperature; phosphorescence spectrum recorded in acetonitrile rigid matrix at 77 K.

1.2.3 Potential Energy Surfaces

The nuclear geometry of a molecule with *N* nuclei is specified by the values of 3*N*-6 internal coordinates, since three of the total of 3*N* degrees of freedom are needed to describe the location of the center of mass and three to describe rotations relative to a laboratory frame. Only the geometry of a diatomic molecule, which is always linear and therefore has only two axes of rotation, is described by 3*N*-5 internal coordinates, i.e. , by the bond length alone.

A collection of 3*N*-6 internal coordinates at a particular geometry represents a point in a 3*N*-6 dimensional mathematical space. A surface produced in a 3*N*-5 dimensional graph in which the total molecular electronic energy of the ground state is plotted against the geometry is known as the ground state potential energy surface. In spite of its name, the total electronic energy contains not only the kinetic and potential energy of the electrons, but also the potential energy of the nuclei. It is not easy to visualize multidimensional potential energy surfaces, and it is customary, albeit frequently misleading, to show limited portions of a surface in two-dimensional(Figure1.7).

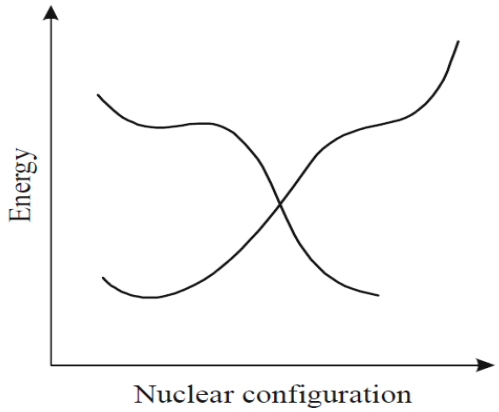

Figure 1.7 Two-dimensional cut through potential energy surfaces (schematic)

The ground state potential energy surface contains minima that correspond to the geometries and energies of more or less stable molecules and can be associated with their chemical (Lewis) structures.

1.2.4 Stokes Shift

Stokes shift is the difference (in wavelength or frequency units) between positions of the band maxima of the absorption and emission spectra (fluorescence and Raman being two examples) of the same electronic transition

(Gispert, 2008) . When a system (be it a molecule or atom) absorbs a photon, it gains energy and enters an excited state. One way for the system to relax is to emit a photon, thus losing its energy (another method would be the loss of heat energy). When the emitted photon has less energy than the absorbed photon, this energy difference is the Stokes shift. If the emitted photon has more energy, the energy difference is called an anti-Stokes shift. (Kitai, 2008)

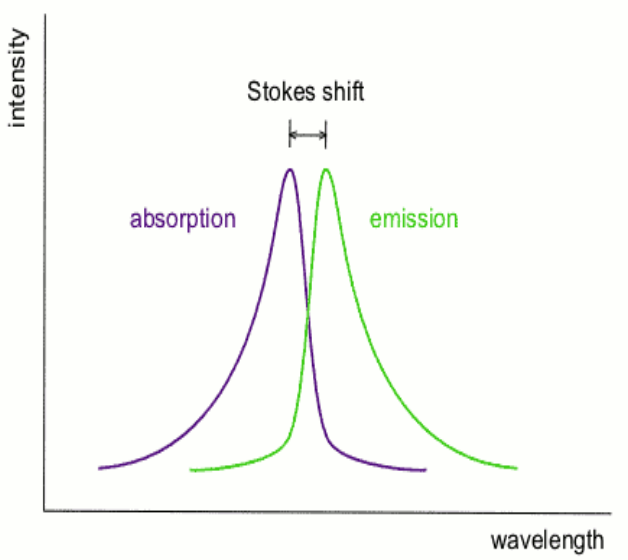

Figure 1.8 The Stokes Shift

1.2.5 Franck-Condon Principle

Radiative transitions may be considered as vertical transitions and may therefore be explained in terms of the Franck–Condon principle. The intensity of any vibrational fine structure associated with such transitions will, therefore, be related to the overlap between the square of the wave functions of the vibronic levels of the excited state and ground state. This overlap is maximized for the most probable electronic transition (the most intense band in the fluorescence spectrum). Figure 1.9 illustrates the quantum mechanical picture of the Franck–Condon principle applied to radiative transitions.

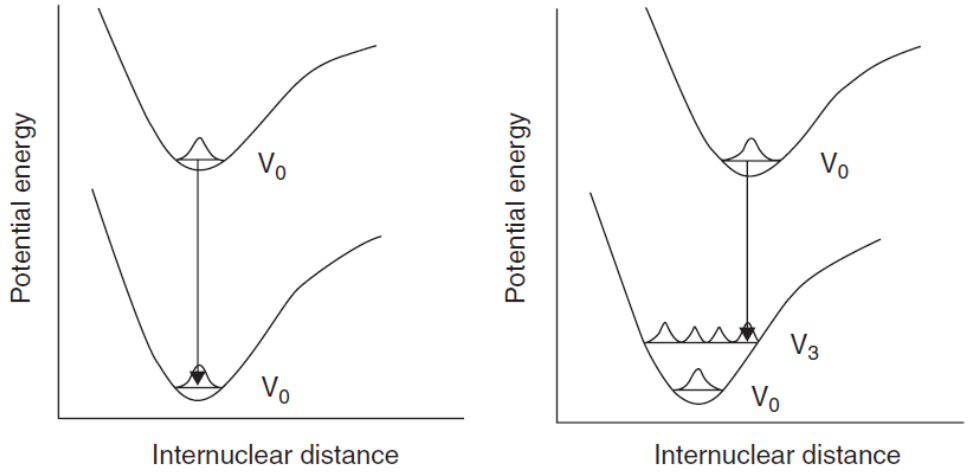

Figure 1.9 Most probable electronic transitions involved in radiative transitions where: (a) both electronic states have similar geometries; (b) the excited state and ground state have very different geometries

1.3 Electronically-Excited States of Molecules

Electronically - excited states of molecules are endowed with excess energy due to their formation by photon absorption. These excited states are short - lived, losing their excess energy within a very short period of time through a variety of deactivation processes (Figure1.10) and returning to a ground–state configuration. If the excited molecule returns to its original ground state then the dissipative process is a physical process, but if a new molecular species is formed then the dissipative process is accompanied by chemical change.

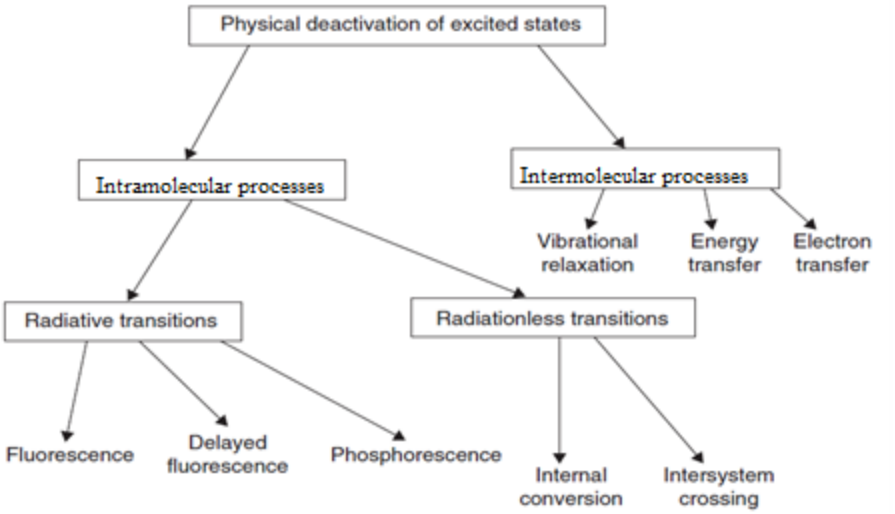

Figure 1.10 Physical deactivation of excited states of organic molecules

1.3.1 Intramolecular processes

Radiative transitions; which involve the emission of electromagnetic radiation as the excited molecule relaxes to the ground state. Fluorescence and phosphorescence are known collectively as luminescence.

Radiationless transitions; where no emission of electromagnetic radiation accompanies the deactivation process.

1.3.2 Intermolecular processes

Vibrational relaxation; where molecules having excess vibrational energy undergo rapid collision with one another other and with solvent molecules to produce molecules in the lowest vibrational level of a particular electronic energy level.

Energy transfer; where the electronically–excited state of one molecule (the donor) is deactivated to a lower electronic state by transferring energy to another molecule (the acceptor), which is itself promoted to a higher electronic state. The acceptor is known as a quencher and the donor is known as a sensitizer.

Electron transfer; considered as a photophysical process, involves a photoexcited donor molecule interacting with a ground - state acceptor molecule. An ion pair is formed, which may undergo back electron transfer, resulting in quenching of the excited donor.

1.4 The Reactions of The Electronically Excited Molecules

For the reaction to be observable by fluorescence measurements, the reaction time be comparable to or shorter than the mean lifetime of the excited molecules. The reactions of the electronically excited molecule can be classified as follows (Weller, 1961).

1.4.1 Quenching of Fluorescence

An excited molecule, A*, loses its energy through interaction with molecule B instead of fluorescence radiation.

$$A^{*} + B \rightarrow (A^{\pm}.B^{\pm} \rightarrow) A + B$$

1.4.2 Complex Formation

An excited form of molecule, A*, can undergo complex formation either with same molecule in ground state, A, or with another molecule, in ground state, B.

$$A^{*} + A \rightarrow A^{*}A$$
$$A^{*} + B \rightarrow A^{*}B$$

1.4.3 Acid-Base Reactions

The acid-base reactions can proceed as follows;

$$A^{*}H + B \rightarrow A^{*} + HB^{+}$$
$$A + HB \rightarrow AH^{+} + B^{-}$$

1.5 The Energy Gap Law

The probability of intramolecular energy transfer between two electronic states is inversely proportional to the energy gap, ΔE, between the two states. The value of the rate constant for radiationless transitions decreases with the size of the energy gap between the initial and final electronic states involved. This law readily provides us with a simple explanation of Kasha's rule and Vavilov's rule. The rate of internal conversion between electronic states is determined by the magnitude of the energy gap between these states. The energy gaps between upper excited states (S_4, S_3, S_2) are relatively small compared to the gap between the lowest excited state and the ground state, and so the internal conversion between them will be rapid. Thus fluorescence is unable to compete with internal conversion from upper excited states. The electronic energy gap between S_1 and S_0 is much larger and so fluorescence ($S_1 \rightarrow S_2$) is able to compete with S_1 (v = 0) $\rightsquigarrow$ S_0 (v = n) internal conversion.

The efficiency of intersystem crossing is determined by the size of the singlet – triplet energy gap (singlet – triplet splitting), ΔE_{ST}. Now, ΔE_{ST} (n, π*) < ΔE_{ST} (π, π*), with ΔE_{ST} (n, π*) being < 60 kJ mol^{-1} and ΔE_{ST} (π, π*) being > 60 kJ mol^{-1}. Therefore intersystem crossing for an (n, π *) excited state will be much faster than intersystem crossing for a (π, π*) excited state (Wiley, 2009).

1.6 Phenomenon of Fluorescence

Luminescence is the emission of light from any substance and occurs from electronically excited states. Luminescence is formally divided into two categories, fluorescence and phosphorescence, depending on the nature of the excited state. In excited singlet states, the electron in the excited orbital is paired (of opposite spin) to the second electron in the ground-state orbital. Consequently, return to the ground state is spin-allowed and occurs rapidly by emission of a photon. The emission rates of fluorescence are typically $10^8 s^{-1}$, so that typical fluorescence lifetime is near 10 ns ($10x10^{-9}$s). Because of the short timescale of fluorescence, measurement of the time-resolved emission requires sophisticated optics and electronics. In spite of the experimental difficulties, time-resolved

fluorescence is widely practiced because of the increased information available from the data, as compared with stationary or steady-state measurements. Phosphorescence is emission of light from triplet excited states, in which the electron in the excited orbital has the same spin orientation as the ground-state electron. Transitions to the ground-state are forbidden and the emission rates are slow (10^3-10^0 s^{-1}) so that phosphorescence lifetimes are typically milliseconds to seconds.

1.6.1 Fluorescence Spectra

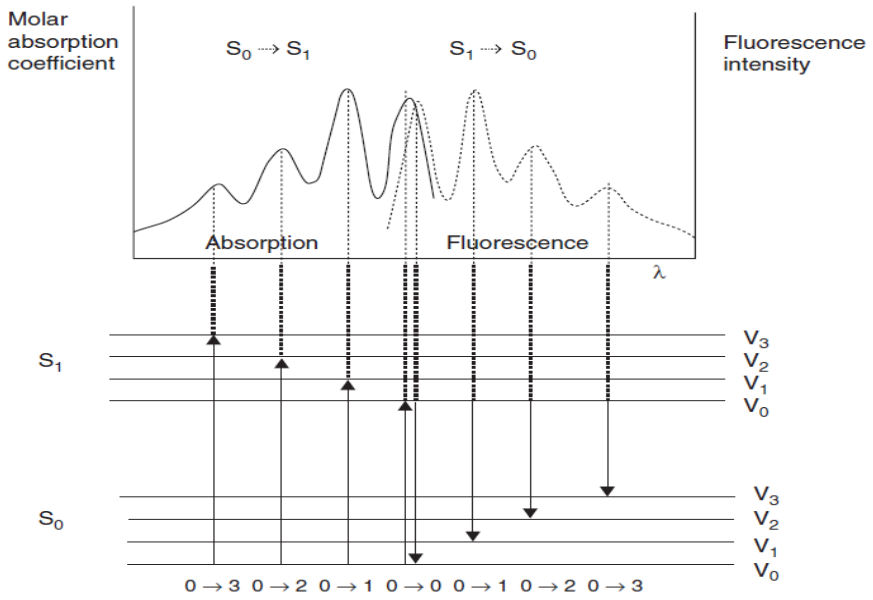

Figure 1.11 Energy - level diagram showing how the electronic and vibrational energy levels in the ground - state (S_0) and first excited - state (S_1) anthracene molecule are related to the absorption and fl uorescence emission spectra

- The 0 – 0 bands for absorption and fluorescence occur at almost the same wavelength.
- Fluorescence emission occurs at longer wavelengths (lower energy) than the 0 – 0 band, while absorption occurs at shorter wavelengths (higher energy) than the 0 – 0 band.
- The absorption spectrum shows a vibrational structure characteristic of the S_1 state whereas the fluorescence spectrum shows a vibrational structure characteristic of the S_2 state of anthracene (Wiley, 2009).

1.6.2 Fluorescence Quantum Yield

The fluorescence quantum yield of a compound may be determined by comparing the area under its fluorescence spectrum with the area under the fluorescence spectrum of a reference compound whose fluorescence quantum yield is known. The spectra of both compounds must be determined under the same conditions in very dilute solution using a spectrometer incorporating a 'corrected spectrum' capability, in order to overcome any variation in detector sensitivity with wavelength.

When a molecule is in the S_1 (v = 0) state, fluorescence emission is only one of the several competing physical processes by which the molecule can return to the ground state. A molecule in S_1 (v = 0) can undergo fluorescence, intersystem crossing or internal conversion, which have rate quantum yields Φ_f, Φ_{isc} and Φ_{ic}, respectively and:

$$\Phi_f + \Phi_{isc} + \Phi_{ic} = 1 \quad (1.3)$$

If the only process occurring from S_1 (v = 0) is fl uorescence then Φ_f will be equal to 1, whereas if no fluorescence occurs from S_1 (v = 0) then Φ_f will be equal to 0. Thus the fluorescence quantum yield has values between 0 and 1. In general, because of the relatively large energy gap between S_0 and S_1, Φ_{ic} is much smaller than Φ_f and Φ_{isc}, which implies that $\Phi_f + \Phi_{isc} \approx 1$ (**Ermolev's rule**) (Wiley, 2009).

1.6.3 Fluorescence Lifetimes

The fluorescence lifetime of a substance usually represents the average amount of time the molecule remains in the excited state prior to its return to the ground state. Lifetime measurements are frequently necessary in fluorescence spectroscopy. These data can reveal the frequency of collisional encounters with

quenching agents, the rate of energy transfer, and the rate of excited state reactions. The precise nature of the fluorescence decay can reveal details about the interactions of the fluorophore with its environment. The measurement of fluorescence lifetimes is difficult because these values are typically near 10 ns, necessitating the use of high-speed electronic devices and detectors. However, because of the importance of these data, a great amount of effort has been directed towards developing reliable means for measurements of fluorescence lifetimes.

There are two widely used methods for the measurements of fluorescence lifetimes. These are the pulse method and the harmonic or phase-modulation method. In the present study, the pulse method has been used. In the pulse method, the sample is excited with a brief pulse of light and the time dependent decay of fluorescence intensity is measured. The method has been explained in detail below (Lakowicz, 1999).

Pulse Lifetime Measurements

Consider the excitation of a fluorophore with an infinitely short pulse of light, resulting in an initial population (N_0) of fluorophores in the excited state.

The rate of decay of the initially excited population is,

$$\frac{dN(t)}{dt} = -(k_r + k_d).N(t) \qquad (1.4)$$

where N(t) is the number of excited molecules at time t following excitation, k_r is the emissive rate, and k_d is the rate of nonradiative decay. Recalling that $N(t)=N_0$ at t=0, integration of the equation (1.4) yields;

$$N(t) = N_0 e^{-t/\tau_0} \qquad (1.5)$$

where $\tau_0 = (k_d + k_r)^{-1}$ is the actual lifetime of the excited state. Hence, we expect the fluorescence intensity I(t), which is proportional to the excited state population $I(t) = k_r.N(t)$, to decay exponentially. The fluorescence lifetime is generally equated with the time required for the intensity to decay to 1/e of its initial value, which is $(k_r+k_d)^{-1}$. Alternatively, the lifetime may be determined from the slope of a plot of the logI(t) versus t.

Measured Lifetimes (τ_0)

If we consider the fluorescence of the S_1 state of M to be in direct competition with internal conversion and intersystem crossing as illustrated in Figure (1.12) or equation (1.6), (1.7) and (1.8)

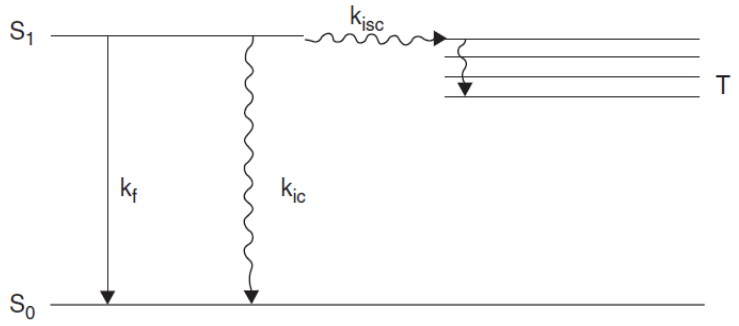

Figure 1.12 Simplified Jablonski Diagram

Reactions	Rates	
$^1M^* \rightarrow M + h\upsilon$	$k_r[M^*]$	(1.6)
$^1M^* \rightarrow {}^3M^*$	$k_{isc}[M^*]$	(1.7)
$^1M^* \rightarrow M$	$k_{IC}[M^*]$	(1.8)

The rate of decay of $[M^*]$ is the given by;

$$-\frac{d[M^*]}{dt} = k_r[M^*] + k_{ISC}[M^*] + k_{IC}[M^*] \quad (1.9)$$

where k_f is the radiative rate coefficient, k_{ISC} is the rate coefficient for intersystem crossing and k_{IC} is the rate coefficient for internal conversion. The decay of $[M^*]$ stil obeys first-order kinetics i.e $[M^*]$ decays exponentially zero with a rate coefficient k_f:

$$[M^*] = [M^*]_0 e^{-k_f t}$$
$$k_f = k_r + k_{ISC} + k_{IC} \quad (1.10)$$

The measured rate coefficient k_f include all of the possible pathways by which M^* may be removed, which can be summarized as $k_f=\Sigma k_i$. The measured fluorescence lifetime (actual lifetime) is thus given by

$$\tau_0 = \frac{1}{k_f} = \frac{1}{\sum k_i} \quad (1.11)$$

1.7 The Effect of The Environment on The Energy States of Molecules

In practice most of chemistry concerns molecules in the condensed phase, as liquids, solids, or more or less in an organized state. The interaction of these condensed phase environments with a molecule is therefore of the greatest importance.

Non-specific Electrostatic Interactions

In a simple model a neutral molecule can be described through two properties related to its electron distribution, the permanent dipole moment μ and the average polarizability α .

For practical purposes the solvent molecules do not appear explicitly in the interaction energy equations; the permanent dipole moments and the polarizabilities of the solvent are expressed as functions of macroscopic properties which are the dielectric constant *D* and the refractive index *n*; the interaction energy is then the product of a quantity which can be described as the solute polarity and another quantity which represents the polarity of the solvent.

Specific Solute-Solvent Associations

In a specific association the molecules form a loose complex, of which hydrogen bonding is the most important example. Hydrogen bonding takes place between a protic (proton donor or acid) molecule such as water and a proton acceptor (base) such as an amine.

The hydrogen bond must be described as a mixture of a covalent bond and a purely electrostatic interaction. It links two molecules in a 1:1 stoichiometry with a fairly well defined bond angle and bond length, subject of course to minor fluctuations. Such specific associations can have important effects on the photophysics and photochemistry of solute molecules, and it must be realized that these interactions depend on the nature of the electronic states; major changes in

hydrogen bonding can take place between the ground state and the excited states of many molecules of importance in biology as well as in industrial applications.

Solvatochromic and Thermochromic Shifts

The solvatochromic shift is the displacement of an absorption or emission band in different solvents.

A thermochromic shift is the displacement of an absorption or emission band with the temperature of the solvent. These displacements result from the change in solvent polarity with temperature, the general rule being that the polarity decreases as the temperature increases. These shifts are small compared with solvatochromic effects and are unlikely to lead to state inversion.

Ion Solvation: The Born Equation

Consider a spherical ion of radius "*a*" which carries a central charge "*q*". The work required to increase this charge by "*dq*" is the potential energy $\left(\frac{q.dq}{a}\right)$ in a vacuum, $\frac{(q.dq)}{Da}$ in a solvent of dielectric constant "*D"*, the difference being the solvation energy. Integration from q=0 to q=(Ze) leads to the Born equation of ion solvation;

$$E = -\left[\frac{(Ze)^2}{2a}\right]F(D) \qquad (1.12)$$

The solvent polarity function $F(D) = \left(1 - 1/D\right)$ having the same saturation property as the Debye and Onsager functions. As *D* goes to infinity all three functions approach the limit of 1 (Suppan, 1994).

1.8 Thermodynamic Investigations

1.8.1 Solvent Effect on Emission Spectra

Emission from fluorophores generally occurs at longer wavelengths than those at which absorption occurs. This loss energy is due to dynamic processes which occur following light absorption.

On the other hand, fluorescence lifetimes are usually longer than the time for solvent relaxation. For that reason, the emission spectra are pattern of the solvent relaxation. However, absorption of light occurs in about 10^{-15} s. This time is too short for motion of the fluorophore or solvent. And this reason can explain why the absorption spectra are less sensitive to solvent polarity than emission spectra(Lakowicz, 1999).

1.8.2. Thermodynamics of chemical reactions

Chemical reactions are one of the main subjects of chemistry. Thermochemistry concerns with properties of reactions. One of them is the probability of formation of reaction, the other is the calculation of energy changes during reaction. Although thermodynamic give information about formation of reaction, it doesn't explain reaction rates. It's interested in only initial and final states.

The importance of the standard enthalpies of formation is that once we know their values, we can calculate the enthalpy of reactions. For example, for the hypothetical reaction,

$$a.A + b.B \rightarrow c.C + d.D$$

where a,b,c and d are stoichiometric coefficients. The enthalpy of reaction carried out under standard state conditions, called the standard enthalpy of reaction, ΔH^0_{rxn}, is given by

$$\Delta H^0_{rxn} = \left[c.\Delta H^0_f(C) + d.\Delta H^0_f(D)\right] - \left[a.\Delta H^0_f(A) + b.\Delta H^0_f(B)\right] \quad (1.13)$$

where a,b,c and d all have the unit mol we can generalize Equation 1.13 as follows;

$$\Delta H^0_{rxn} = \Sigma n \Delta H^0_f(\text{products}) - \Sigma m \Delta H^0_f(\text{reactants}) \tag{1.14}$$

where m and n represent the stoichiometric coefficients for the reactants and products, and Σ (sigma) means "the sum of".

Having established thermodynamic relationships for deriving the electromotive forces of reductions and oxidations of excited state donor and acceptor molecules and calculating the free energy change accompanying excited states electron transfer, a useful expression is given. Figure 1.13 shows a thermodynamically uphill pathway involving D and A as well as a downhill pathway from D^* and A. The overall free-energy change for the uphill process is equal to the sum of the free energy changes for oxidation of the donor and reduction of the acceptor:

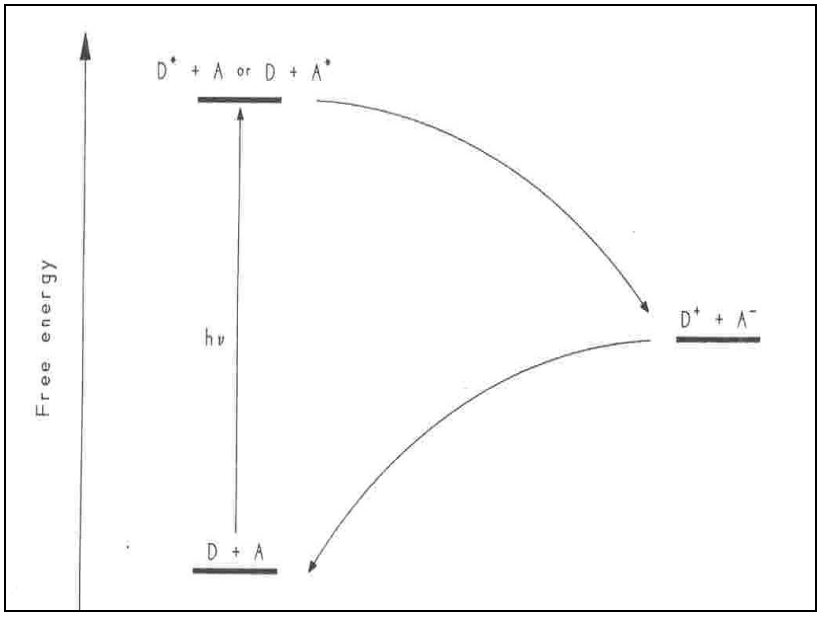

Figure 1.13 An archetypal energy diagram for photoinduced electron transfer

$$\Delta G_{el} = \Delta G_{D/D^+} + \Delta G_{A/A^-} \quad (1.14)$$

where ΔG_{el} specifies the standard free-energy change.

$$\Delta G_{el}(eV) = nF(-E_{D/D^+} - E_{A/A^-}) \quad (1.15)$$

or ,in keeping with the convention of writing all half-reactions as reductions and using redox potential :

$$\Delta G_{el}(eV) = nF[E^0(D^+/D) - E^0(A/A^-)] \quad (1.16)$$

The free-energy change for an electron transfer between an excited donor and ground-state acceptor the thermodynamically downhill reaction can be derived in a similar manner:

$$\Delta G_{el}(eV) = nF[E^0(D^+/D^*) - E^0(A/A^-)] \quad (1.17)$$

The substitution is given as;

$$\Delta G_{el}(eV) = nF[E^0(D^+/D) - E^0(A/A^-) - \Delta G_{00}] \quad (1.18)$$

where ΔG_{00} is the free in electron volts corresponding to the equilibrium energy, E_{00}. For most one-electron transfers, N_f is nearly equal to 1, so that we can write

$$\Delta G_{el}(eV) = E^0(D^+/D) - E^0(A/A^-) - \Delta G_{00} \quad (1.19)$$

If we measure the excited-state energy in kilocalories per mole and redox potentials in volt, as is customary, equation (1.18) can be written as

$$\Delta G_{el}(kcalmol^{-1}) = 23{,}06[E^0(D^+/D) - E^0(A/A^-)] - \Delta G_{00} \qquad (1.20)$$

A similar treatment applied to the electron transfer between A^* and D also leads to equation 1.20

To apply equation 1.20, the only experimental parameters required are the excited-state energy of the photoexcited molecule and the redox potentials of the ground states of both the electron donor and acceptor. A point worth noting is that equation 1.20 is applicable to an equilibrated excited state and not to a Franck-Condon state. The electron transfer occurs after the equilibration of the Franck-Condon excited state to the relaxed, equilibrated state. This should not be taken to mean that electron transfer cannot take place in systems involving unrelaxed excited states. There are, in fact, examples in the literature describing electron transfer in these cases, but we will not consider them in this writing.

There is an important refinement that can be introduced into equation 1.20. Suppose for now that the donor and acceptor are neutral molecules. Electron transfer would then generate two charged species-D^+ and A^-. When this ion pair is formed, attractive Coulombic forces will draw the two ions closer together and result in a release of energy. This attraction is given by a work term, w_p, derived from Coulomb's Law.

$$w_p(kcalmol^{-1}) = \frac{(z_d^+ z_a^-)e^2}{d_{cc}e_s} = \frac{332(z_d^+ z_a^-)}{d_{cc}e_s} \qquad (1.21)$$

where z_D^+ and z_A^- are the charges on the molecules, e_s is the static dielectric constant of solvent, and d_{cc} is the center-to-center separation distance in Angstrom (A^0) between the two ions.

$$\Delta G_{el}(kcalmol^{-1}) = 23{,}06[E^0(D^+/D) - E^0(A/A^-)] - w_p - \Delta G_{00} \qquad (1.22)$$

which is called the Rehm-Weller equation. According to the work term in equation 1.22, the presence of electrostatic interactions between the ions should influence the free-energy change accompanying electron transfer. Under polar conditions where e_s is large (e.g., e_s=37 for acetonitrile), w_p ~1.3 kcalmol^{-1} for the usual case where z_D^+=+1 and d_{cc} ~ 7 A^0. When using equation 1.22 to calculate ΔG_{el} for a reaction in a given solvent, the choice of redox potentials is important. Preferably, they should be measured in the same solvent or in a solvent with a similar dielectric constant. Since most of the redox potentials have been measured in polar solvents, the use of these redox potentials to calculate ΔG_{el} in nonpolar media may lead to erroneous values. Equation 1.22 can be modified to calculate free energies in nonpolar solvents using redox potentials measured in polar media.

At the heart of electron photochemistry, equation 1.22 states concisely the fundamental thermodynamic condition for spontaneous electron transfer between neutral reactants: $\Delta G_{el}<0$ (Kavarnos, 1993).

1.9 Kinetic Investigation

1.9.1 Fluorescence Quenching: Stern Volmer Equation

The lifetime of the induced molecule (sensitizer) must be sufficiently long to ensure the electron transfer. The electron transfer mechanism and quenching speed constant k_q of one electron donor or acceptor can be found by the measured singlet lifetime in several quencher concentrations. The Stern-Volmer equation corresponds this situation:

$$\frac{1}{\tau_f} - \frac{1}{\tau_f^0} = 1 + k_q[Q] \qquad (1.23)$$

τ_f and τ^0_f are respectively the fluorescence lifetimes when there is a quencher and there is not a quenching. τ_f decreases if more quenching are added. k_q is obtained from the grade of the graphic which is drawn between $1/\tau_f$ and [Q]. When k_q is about 10^9-10^{10} $M^{-1}s^{-1}$ degree, the reaction is too fast so the diffusion is controlled (under control). So the step, which determines te speed, is the part in which the molecule (sensitizer) quencher drop in diffusion.

When continuous condition circumstance is applied,

$$k_q = \frac{k_{diff}}{1+(k_{diff}/k_{el})[1+(k_{-el}/k_{ret})]} \tag{1.24}$$

is obtained. The equation is simplified by assuming $k_{ret}>>k_{el}$. In the other assumption, backward electron transfer k_{-el} generally thermodynamically the energy barrier is higher but to turning back to the ground state is easier thermodynamically.

In this condition the equation is:

$$k_q = \frac{k_{diff}.k_{el}}{k_{el}+k_{-diff}} \tag{1.25}$$

For fast electron transfer condition the reactants are diffused through each other if every action is a reaction, $k_{diff}>>k_{el}$ and $k_q=k_{diff}$. Reaction is diffusion controlled.

Fluorescence quenching refers to any process which decreases the fluorescence intensity of a given substance. A variety of processes can result in quenching. These include excited state reactions, energy transfer, complex formation, and collisional quenching. Both static and dynamic quenching require molecular contact between the fluorophore and quencher. In the case of collisional quenching, the quencher must diffuse to the fluorophore during the lifetime of the excited state. Upon contact, the fluorophore returns to the ground state without

emission of a photon. The magnitude of fluorescence quenching depends on both acceptor and solvent.

Quenching measurements can reveal the accessibility of fluorophores to quenchers. If a given solvent is very viscous, then diffusion is slow and quenching is inhibited. Hence, quenching can reveal the diffusion rates of quenchers. Furthermore, fluorescence efficiency can be lower with increasing acceptor concentration.

Fluorescence quenching has been described by Stern-Volmer Equation. Considering the ratio of the quantum yields.

$$\Phi_Q = \frac{k_r}{\Sigma k_i + k_q[Q]} \tag{1.26}$$

With the rate constant k_1 and using Equation (1.14) yield

$$\frac{\Phi_f}{\Phi_Q} = \frac{\Sigma k_i + k_q[Q]}{\Sigma k_i} = 1 + k_q[Q]\tau_0 \tag{1.27}$$

where [Q] is the quencher concentration instead of quantum yields, the fluorescent intensities in the absence (I_f) and presence quencher I_Q be written taking into account dynamic quenching constant

$K_{sv}=k_q\tau_0$

And hence reforming equation give;

$$\frac{I_f}{I_Q} = 1 + K_{SV}[Q] \tag{1.28}$$

which is the Stern-Volmer equation.

The graph drawn between $\left[\left(I_f / I_Q\right) - 1\right]$ and [Q] gives a straight line with the slope K_{SV} and substitution the actual fluorescence lifetime for τ_0 in equation (1.28) gives the rate constant k_q.

If complex formation between donor and acceptor in charge-transfer transition interaction takes place in the excited state not in the ground state this complex is named as “exciplex” and the corresponding band can be seen in emission spectrum (Weller, 1961).

Exciplex formation in the excited state and quenching of fluorescence between aromatic compounds and aromatic or aliphatic amines can be investigated. In nonpolar solvent, the kinetics of exciplex formation and disappearance follow the kinetics in Scheme 1.1 below;

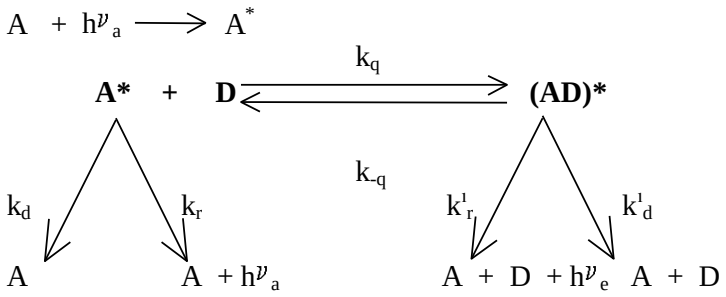

Scheme 1.1 Scheme of the kinetics of exciplex formation and disappearance

In the complex formation in excited state, the acceptor (A) is an aromatic hydrocarbon molecule and the donor (D) an amine. Within the framework of this scheme, fluorescence quantum yields and fluorescence decay parameters can be derived (Palmas et al., 1984, Swinnen et al., 1987). The rate constant for exciplex formation (k_q) was diffusion controlled while that for exciplex dissociation was negligibly small. The rate constant for exciplex formation can be calculated from Stern-Volmer quenching constant (K_{SV}) by equation (1.27).

Exciplex formation between aromatic molecule and amine has been studied as a function of temperature and solvent and exciplex stabilization enthalpy, ΔH, can be obtained (Khalil et al., 1993).

1.9.2 Exciplexes

If two molecules form a complex in the excited state called as exciplex (excited complex) but not in the ground state. These type of complexes became because of the diffusional quenching of two molecules and called encounter complexes. As a result the charge distribution shifts from the donor molecule to the acceptor the acceptor and called the intermolecular electron transfer. Wavefunction for the excimer has been formed by the overlapping of the wavefunctions of molecules and charge separated forms as;

$$\left|\psi_{ex}\right\rangle = \alpha\left|\psi_{D^*A}\right\rangle + \beta\left|\psi_{D^+A^-}\right\rangle + \gamma\left|\psi_{DA^*}\right\rangle \tag{1.29}$$

Exciplexes with a close charge separation can be explained as positive charge on donor and negative charge on acceptor are localized (β>α). Charge separation has been seen by the nonradiative transition or emission (exciplex fluorescence) in nonpolar solvents. It can be usually separated in solvated radical ion forms in more polar solvents.

The molecules came close to each other by diffusion and formed an encounter complex before the electron transfer in the intermolecular systems. As shown Figure 1.14 excitation of an electron acceptor, electronically excited form of A^* has been formed. The donor D and acceptor in the ground state came close to each other diffusionally during the lifetime of A^*. Finally the charge transfer has been achieved by the collisional complex $(AD)^*$. As a result $(A^-D^+)^*$ exciplex has been obtained. This complex depends on the donor and acceptor molecules and the solvents as with CRIP (contact radical ion pair) or SSRIP (solvent separated radical ion pair). Exciplex emission maximum is shifted compared with that of the monomer emission and shows the solvatochromism.

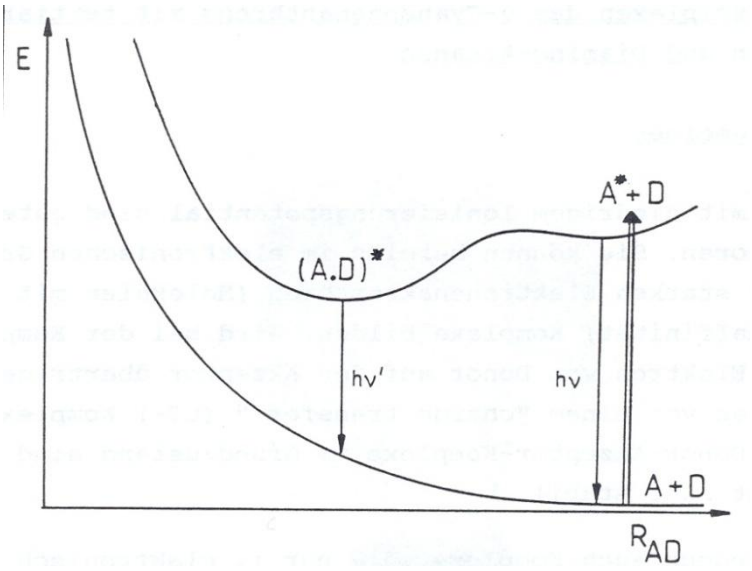

Figure 1.14 Potential energy diagram for the exciplex formation and decay

The chemical association of the exciplex results from an attraction between the excited - state molecule and the ground - state molecule, brought about by a transfer of electronic charge between the molecules. Thus exciplexes are polar species. Evidence for the charge - transfer nature of exciplexes in nonpolar solvents is provided by the strong linear correlation between the energy ofthe photons involved in exciplex emission and the redox potentials ofthe components. The exciplex emission is also affected by solvent polarity, where an increase in the solvent polarity results in a lowering of the energy level of the exciplex, at the same time allowing stabilization of charged species formed by electron transfer (Figure1.14). Thus, in polar solvents the exciplex emission is shifted to even higher wavelength and accompanied by a decrease in the intensity of the emission, due to competition between exciplex formation and electron transfer (Blackwell, 1991

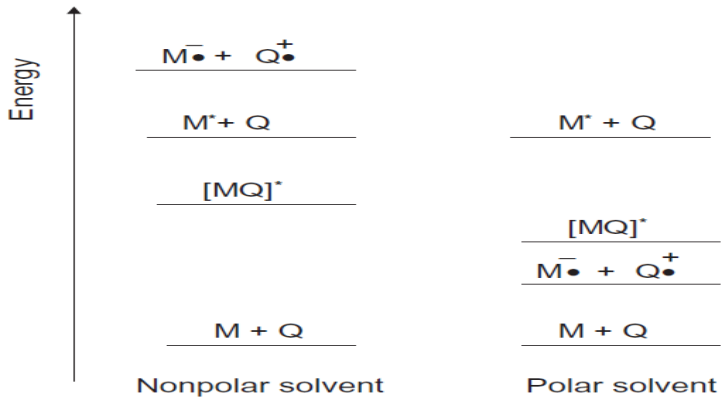

Figure 1.15 Energy diagram for exciplex formation in solvents of differing Polarities(M*=excited molecule, Q=quencher in ground state)

1.9.3 Theory of Static and Dynamic Quenching

The quenching that resulted from diffusive encounters between the fluorophore and quencher during the lifetime of the excited state is a time-dependent process. Quenching can also occur as a result of the formation of a nonfluorescent complex between the fluorophore and quencher. When this complex absorbs light, it immediately returns to the ground state without emission of a proton. The dependence of the fluorescence intensity upon quencher

concentration for static quenching is easily derived by consideration of the association constant for complex formation. This constant is given by;

$$K_S = \frac{[F-Q]}{[F][Q]} \tag{1.30}$$

where [F-Q] is the concentration of the complex, [F] is the concentration of uncomplexed fluorophore, and [Q] is the concentration of quencher. If the complexed species is nonfluorescent, then the fraction of the fluorescence that remains, I/I_0 is given by the fraction of the total fluorophores that are not complexed , $F = I/I_0$. Recalling that the total concentration of fluorophore , $[F]_0$, is given by;

$$[F]_0 = [F] + [F-Q] \tag{1.31}$$

substitution into equation (1.30) yields;

$$K_S = \frac{[F-Q]}{[F][Q]} = \frac{[F]_0}{[F][Q]} - \frac{1}{[Q]} \tag{1.32}$$

We can substitute fluorescence intensities for the fluorophore concentrations, and rearrangement of equation (1.32) yields;

$$\frac{I}{I_0} = 1 + K_S[Q] \tag{1.33}$$

Note that the dependence of I_0/I on [Q] is linear and is identical to that observed for dynamic quenching except that the quenching constant is now the association constant. Unless additional information is provided, fluorescence quenching data obtained by intensity measurements alone can be explained by either a dynamic or a static process. As will be shown below, the magnitude of K_S can sometimes be used to demonstrate that dynamic quenching cannot account for the decrease in intensity. The measurement of fluorescence lifetimes is the most definite method to distinguish static and dynamic quenching. Static quenching removes a fraction of the fluorophores from observation. The complexed fluorophores are nonfluorescent, and the only observed fluorescence is from the un-complexed fluorophores. The uncomplexed fraction is unperturbed, and hence

the lifetime is τ_0. Therefore, for static quenching $\tau_0/\tau = 1$. In contrast, for dynamic quenching, $\tau_0/\tau = I_0/I$.

Besides measurement of fluorescence lifetimes, static and dynamic quenching can often be distinguished on the basis of other considerations. Dynamic quenching depends upon diffusion. Since higher temperatures result in larger diffusion coefficients, the bimolecular quenching constants are expected to be increase with increasing temperature. More specifically, kq is expected to be proportional to T/η since diffusion coefficients are proportional to this ratio in contrast, increased temperature is likely to result in decreased stability of complexes, and thus lower values of the static quenching constants. One additional method to distinguish static and dynamic quenching is by careful examination of the absorption spectra of the fluorophore. Collisional quenching only affects the excited states of the fluorophores, and thus no changes in the absorption spectra are expected. In contrast, ground-state complex formation will frequently result in perturbation of the absorption spectrum of the fluorophore, in fact, a more complete form of equation 1.31 would include the possibility of different extinction coefficients for free and complexed forms of the fluorophore (Lakowicz, 1999).

2. COMPUTATIONAL METHODS

Chemistry is the science dealing with construction, transformation and properties of molecules. Theoretical chemistry is the subfield where mathematical methods are combined with fundamental laws of physics to study processes of chemical relevance. Molecules are traditionally considered as “composed” of atoms or, in a more general sense, as a collection of charged particles, positive nuclei and negative electrons. The only important physical force for chemical phenomena is the Coulomb interaction between these charged particles. Molecules differ because they contain different nuclei and numbers of electrons, or because the nuclear centers are at different geometrical positions.

Given a set of nuclei and electrons, theoretical chemistry can attempt to calculate things such as:

• Which geometrical arrangements of the nuclei correspond to stable molecules?
• What are their relative energies?
• What are their properties (dipole moment, polarizability, NMR coupling constants, etc.)?
• What is the rate at which one stable molecule can transform into another?
• What is the time dependence of molecular structures and properties?
• How do different molecules interact?

Computational chemistry is focused on obtaining results relevant to chemical problems, not directly at developing new theoretical methods. There is of course a strong interplay between traditional theoretical chemistry and computational chemistry. Developing new theoretical models may enable new problems to be studied, and results from calculations may reveal limitations and suggest improvements in the underlying theory. Depending on the accuracy wanted, and the nature of the system at hand, one can today obtain useful information for systems containing up to several thousand particles. One of the main problems in computational chemistry is selecting a suitable level of theory for a given problem, and to be able to evaluate the quality of the obtained results (Wiley, 2007). The computational methods are classified in two main groups: force field (MM) calculations and electronic structure methods. And electronic structure methods also consist semiempirical methods, ab-initio and DFT methods.

2.1 Molecular Mechanics Methods

Molecular mechanics (MM) simulations use the laws of classical physics to predict the structures and properties of molecules. The term molecular mechanics implies that Newton's mechanics will be used for the modeling of a molecular system. The molecular mechanics potential energy of the entire system is calculated using a force field. There are many different molecular mechanics methods. And each one is characterized by its particular force field. Molecular

mechanics calculations do not explicitly treat the electrons in a molecular system. This method achieves calculations depending on the interactions among the nuclei. Electronic effects are implicitly included in force fields through parameterization. MM is typically applied to large biological systems or other systems containing large amounts of atoms, rather than small molecules. In other words, in many cases, large molecular systems can be modeled successfully by using the MM method. The harmonic oscillator expression is used within the MM model to obtain compound energies. All the parameter constants in these equations are required; otherwise ab initio calculations are obtained.

According to MM, total energy of molecules is showed that;

$$E_{tot} = E_{bond}(R_{AB}) + E_{angels}(\theta_{ABC}) + E_{torsion}(\phi_{ABCD}) + E_{vdw}(R_{AB}) + E_{coulomb}(R_{AB}, Q_A, Q_B) \quad (2.1)$$

E_{tot}: total energy

E_{bond}, E_{angels}, $E_{torsion}$: Bonded interactions, depend on atoms that are connected to each other

E_{vdw}, $E_{coulomb}$: Non-bonded interactions, depend on atoms that are not connected to each other

R_{AB}: Distance between atoms A and B

θ_{ABC}: Angle formed by atoms A,B and C

ϕ_{ABCD}: Torsional angel formed by atoms A,B,C and D

2.2 Electronic Structure (Quantum Mechanical) Methods

Electronic structure methods use the laws of quantum mechanics for their computations. Wave functions are used to describe the state of a system in quantum mechanics an they are donated by Ψ . The wave function depends only on the spatial coordinates of the system and time. The properties of a system are usually time independent or time averaged. For a complete description of an atom, the Schrödinger Equation which includes the relations of the electrons with the nucleus among themselves is used;

$$H\Psi = E\Psi \tag{2.2}$$

H= Hamiltonian operator of the system under observation

Ψ = Wavefunction

E= Total energy of the system

The Hamiltonian operator is used to calculate energies (Eigen values) and the wave function which is an Eigen function of the operator H.

For any but the smallest systems however, exact solutions to the Schrödinger equation are not computationally practical. Electronic structure methods are characterized by their various mathematical approximations to its solution. Born-Oppenheimer is one the approximations where the coupling between the nuclei and electronic motion is neglected. Electron move faster with respect to the nuclei which have larger mass; so, nuclei can see an averaged potential of electrons whereas electrons can see any positional change in nuclei. It can be separated into nuclear and electronic wave functions as in the equation.

$$H = T_n + T_e + V \tag{2.3}$$

$$\Psi = \Psi_n + \Psi_e \tag{2.4}$$

Hamiltonian is shown in Eq (2.3) T_n denotes the kinetic energy of the nuclei, T_e stands for the kinetic energy of the electrons and V represents the potential energy. The nuclei move slower than the electrons, the kinetic energy of the nuclei can be neglected and the repulsion between the nuclei can be considered to be constant during the optimization (Born-Oppenheimer Approximation) (Levine, 1991).

Another significant simplification can be obtained by introducing independent-particle models, where the motion of one electron is considered to be independent of the dynamics of all other electrons. This model means that the interactions between the particles are approximated, either by neglecting all but the most important one, or by taking all interactions into account in an average fashion. Within electronic structure theory, only the latter has an acceptable accuracy, and is called Hartree-Fock(HF) theory. In the HF model, each electron is described by an orbital, and the total wave function is given as a product of orbitals.

2.2.1 Semi-Empricial Methods

Semi-empirical quantum chemistry methods are based on the Hartree-Fock formalism, but make many approximations and obtain some parameters from empirical data. They are very important in computational chemistry for treating large molecules where the full Hartree-Fock method without the approximations is too expensive. The use of empirical parameters appears to allow some inclusion of electron correlation effects into the methods.

Semi-empirical methods follow what are often called empirical methods where the two-electron part of the Hamiltonian is not explicitly included. For π-electron systems, this was the Hückel method proposed by Erich Hückel (Hückel, 1978). For all valence electron systems, the Extended Hückel method was proposed by Roald Hoffmann (Hoffmann, 1963).

Semi-empirical calculations are much faster than their ab initio counterparts. Their results, however, can be very wrong if the molecule being computed is not similar enough to the molecules in the database used to parameterize the method.

2.2.2 Ab-Initio Methods

Ab-initio electronic structure calculations, ("ab-initio" is Latin and means "first principles"), are based on the Schrödinger equation. One of the most fundamental equations of modern physics, this equation can identify many things including the behavior of electrons in molecules. Ab-initio methods are provided to approximately solve the Schrödinger equation and to obtain the wave function and energy of a molecule. The wave function is a mathematical function used to calculate the electron distribution and contains all information required to describe that state. Electron distribution within a molecule is polar, and ab-initio calculations can elucidate which parts of the molecule are electrophilic or nucleophilic. However, the Schrödinger equation, except for single-electron system, is not analytically solvable. Therefore, various approximations for the solution of the Schrödinger equation are considered high-level ab-initio methods. Regardless of the level, all ab-initio quantum mechanical methods base on fundamental physical theories and not semi-empirical parameterizations. The calculations are made starting from first principles. Therefore, ab-initio methods, compared to the MM and semi-empirical methods are much slower and

computationally intensive. Of the ab-inito methods, Hartree-Fock (HF), Multi-configurational self-consistent field (MCSCF), many body perturbation theory (MBPT), configuration interaction (CI), and linked stack (coupled-cluster, CC) methods (Besides simple HF, all methods take into account the energy of electron correlation) can be regarded as the most important.

2.2.3 Density Functional Theory (DFT) Methods

Density functional theory (DFT) has become very popular in recent years. This is justified based on the pragmatic observation that is less computationally intensive than other methods with similar accuracy. This theory has been developed more recently than other ab-initio methods. Because of this, there are classes of problems not yet explored with this theory, making it all the more crucial to test the accuracy of the method before applying it to unknown systems.

DFT methods such as ab-initio methods and SE are based on the solution of the Schrödinger equation By DFT methodologies. In contrast to the previously described methods, the wave function describing the electron probability distribution is calculated exactly. DFT methods can be considered among the ab-initio techniques, although more complex calculations can be conducted using empirical parameterizations (meta-GGA for example). This blending of empirical and ab-initio techniques has led to a classification scheme known as Jacob's ladder, in which techniques higher up the ladder include more energy terms or the addition of exchange correlation from other techniques. In DFT methods, energy is calculated often according to the Kohn-Sham (KS) scheme, in which one particle KS energies and Hamiltonians depend upon density through the unique local one particle potential. DFT methods, compared with other high-level ab-initio methods, can deliver high-quality results with relatively short calculation times, especially when using resolution of the identity (RI) methods. DFT results can only be improved by using larger basis sets. The main challenge in DFT is to choose the appropriate functional for the system under investigation.

The excited states of polycyclic aromatic hydrocarbons (PAH) with up to 28 π-electrons have been investigated in the framework of time-dependent density functional theory (TD-DFT). The density functional formalism of Hohenberg (Hohenberg, 1964) and Kohn and Sham (Kohn, 1965) has become an effective tool in computational chemistry to determine a variety of ground state properties

of molecules. As density functional theory (DFT) has been recognized as an inexpensive and reasonably perfect method that resolves many problems of the Hartree-Fock (HF) approximation, there has been a great interest to extend the DFT approach to excited electronic states. In our day the most successful and widely used method to calculate excitation energies and electronic spectra is the time-dependent generalization of DFT theory (TD-DFT) (Gross et al., 1996; Casida, 1995; Bauernschmitt and Ahlrichs, 1996; Görling et al., 1999 and Furche, 2001). Additionally, in this present work, two popular hybrid functionals, namely B3LYP (Becke, 1993 and Lee et al., 1988) and PBE1PBE (Perdew et al., 1996) have been used, because they already showed a wide applicability for different kinds of molecular systems. The benchmark study of Zhao and Truhlar (Zhao and Truhlar, 2005) concerning DFT performances on describing nonbonded interactions points out that the B3LYP hybrid density functional, widely accepted as the standard DFT method, describes the nonbonded interactions rather poorly, while the PBE1PBE functional is one of the best methods describing these types of interactions. Therefore, we mainly exploited the PBE1PBE hybrid functional for all ground state geometry optimizations and frequency calculations.

3. EXPERIMENTAL

3.1 Apparatus

The following methods were used for the investigation of absorption and emission spectra. Preliminary the donor and acceptor solutions were optimized by recording the absorption and emission data at λ_{max} for a series of selected donor and acceptor solutions in varying concentrations.

3.1.1 UV-VIS Spectroscopy

All the absorbance measurements were taken using Perkin Elmer-Lambda35 UV-visible Spectrophotometer. The thickness of quartz cuvette is 1 cm.

3.1.2 Steady-State Fluorescence Spectroscopy

Steady-state measurements were performed by Perkin Elmer LS-55 Spectrofluorophotometer. During measurements of fluorescence intensities and lifetimes, nitrogen gas applied to remove the dissolved oxygen in the solution so that quenching effect due to presence of oxygen was disappeared.

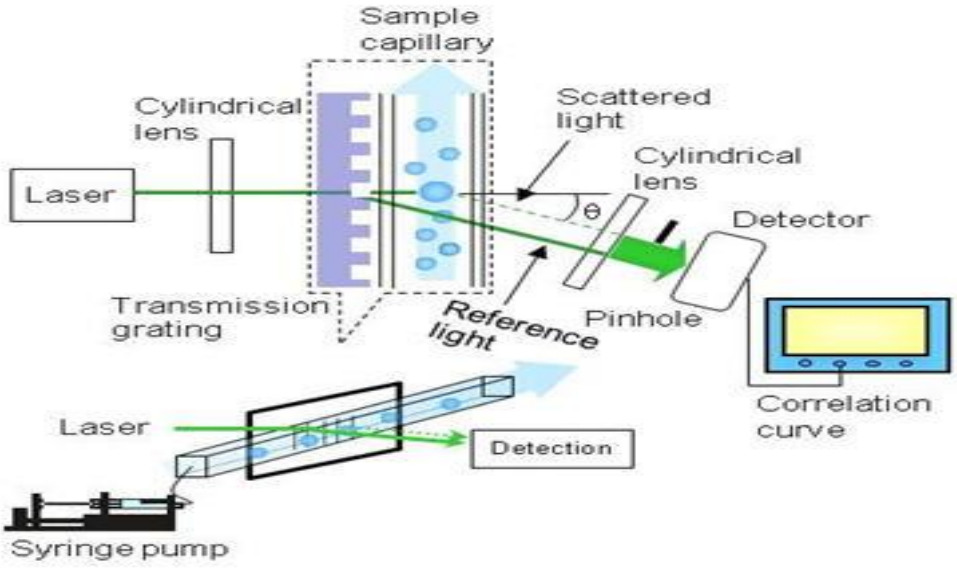

Figure 3.1 Steady state fluorescence spectroscopy

3.2 Reagents and Solutions

The properties of the used donor and acceptor systems are as follows: protoporphyrin(IX) (95 %, Sigma-Aldrich), Pyrene (99 %, Fluka), 1-Hydroxypyrene (98 %, Sigma-Aldrich); solvent systems chosen are

dichloromehthane (99,9 %, Merck), tetrahydrofuran (99,9 %, Merck) and 2-methyl tetrahydrofuran (99,9 %, Sigma-Aldrich).

Acceptors:

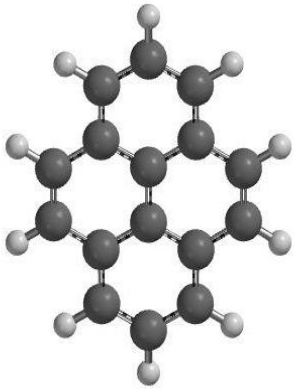

Pyrene (py)

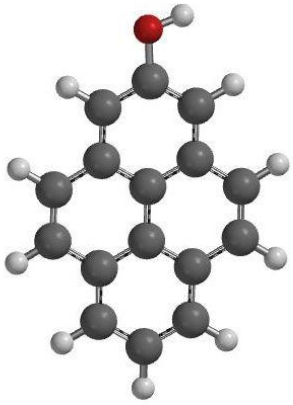

1-hydroxypyrene (pyOH)

Donor:

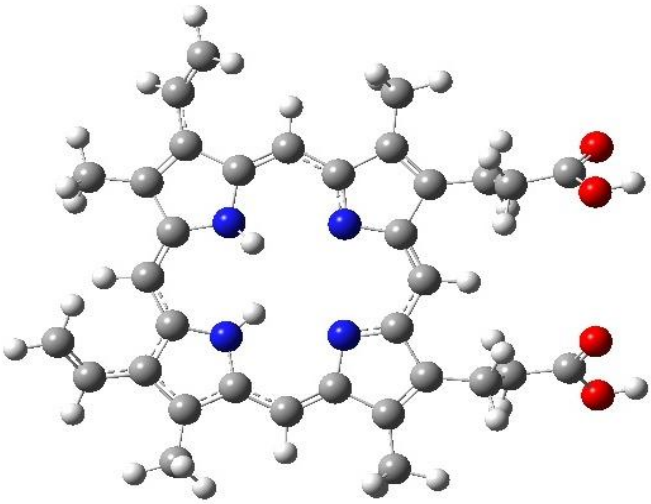

Protoporphyrin (IX) (protoporp)

3.3 Quantum Chemical Calculation

Initial ground state geometries of donor-acceptor complexes were obtained by utilizing conformational analysis. In this analysis, mainly acceptor molecule was held fixed and the minimum energy structure was obtained by determining the energy alteration via change in the orientation of donor molecule with respect to the acceptor. After obtaining their initial geometries, all of these geometries were optimized at PBE1PBE/6-31G(d) level of theory by utilizing Gaussian98 computational chemistry suite (Frisch et al.). The vertical excitation energies of these complexes were obtained single point time dependent density functional

theory methods. Particularly, TD-PBE1PBE/6-31G(d) method was employed throughout the study.

4. RESULTS AND DISCUSSION

4.1 Spectrophotometric Investigation

4.1.1 Pyrene-Protoporphyrin (IX) System

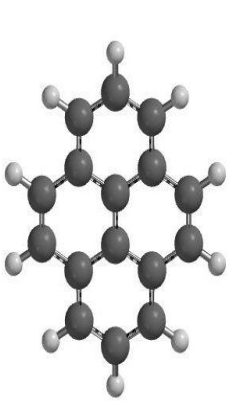

Pyrene

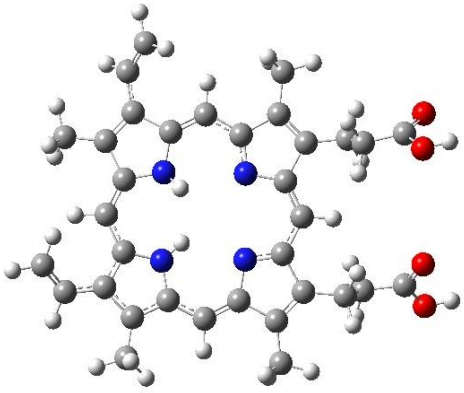

Protoporphyrin(IX)

Figure 4.1 Geometric structures of pyrene and protoporphyrin with minimum energy calculated by AM1

Figure 4.2 displays the UV-Vis spectra of pyrene and protopophyrin(IX) in DCM. The characteristic peaks of protoporphyrin are observed 407, 545 and 569 nm. In pyrene-protoporphyrin system, the measurements are repeated by using different concentrations. The concentration of pyrene is nearly 10^{-5} M and the concentration of protoporphyrin is changed between $3.5x10^{-6}$ M and $2.5x10^{-5}$ M. Absorption spectra of this system have shown in Figure 4.3.

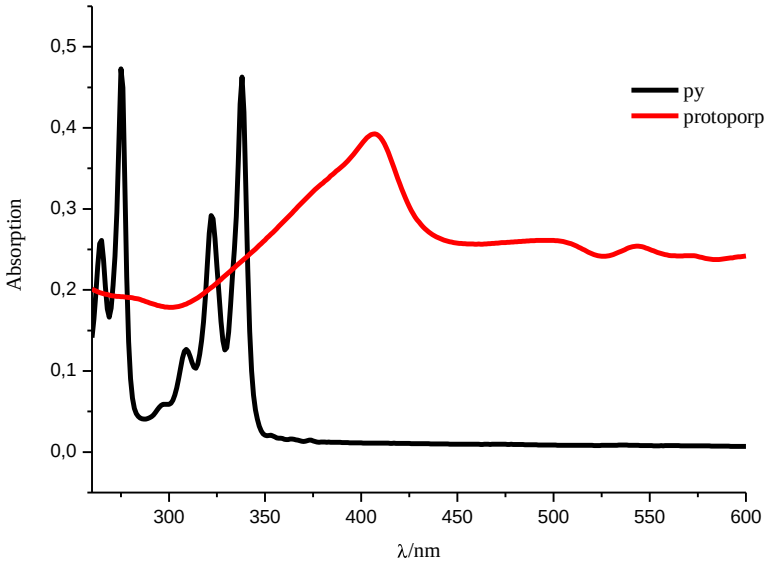

Figure 4.2 UV-Vis spectra of pyrene and protoporphyrin in DCM

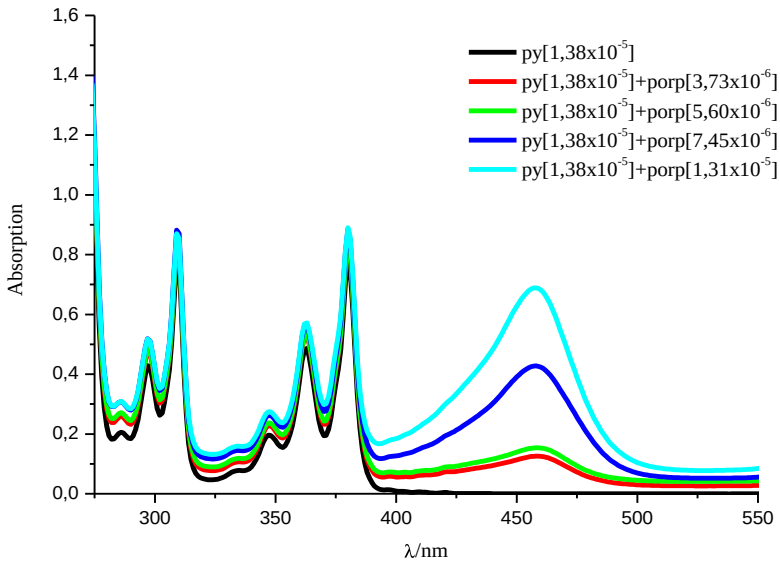

Figure 4.3 UV-Vis spectra of pyrene-protoporphyrin system in DCM

The absorption spectra of pyrene are measured between 260 and 550 nm. 371 nm shows that 0-0 transition but it is not clear. Second electronic excited state have been seen at 334 nm($S_0 \rightarrow S_2$). Second and third(271 nm) excited state transitions are show clearly itself in vibrational structure. During the measuruments, the concentrations of protoporphyrin are increased and the measurements are repeated. However, the absorption spectra of pyrene are not changed with addition of protoporphyrin except absorption intensity.

From this, it is concluded that there isnt any interactions between pyrene and protoporphyrin in the ground state.

The fluorescence measurements of pyrene-protoporphyrin system have been taken in several solvents with medium polarity. In particular, dichloromethane (DCM), tetrahydrofuran (THF) and 2-methyl tetrahydrofuran (2Me-THF) were used as solvents. The excitation wavelength is chosen at 337 nm from absorption spectra. At this excitation wavelength, there is scarcely any intensity of protoporphyrin. So, only pyrene (acceptor) has been excited at this wavelength.

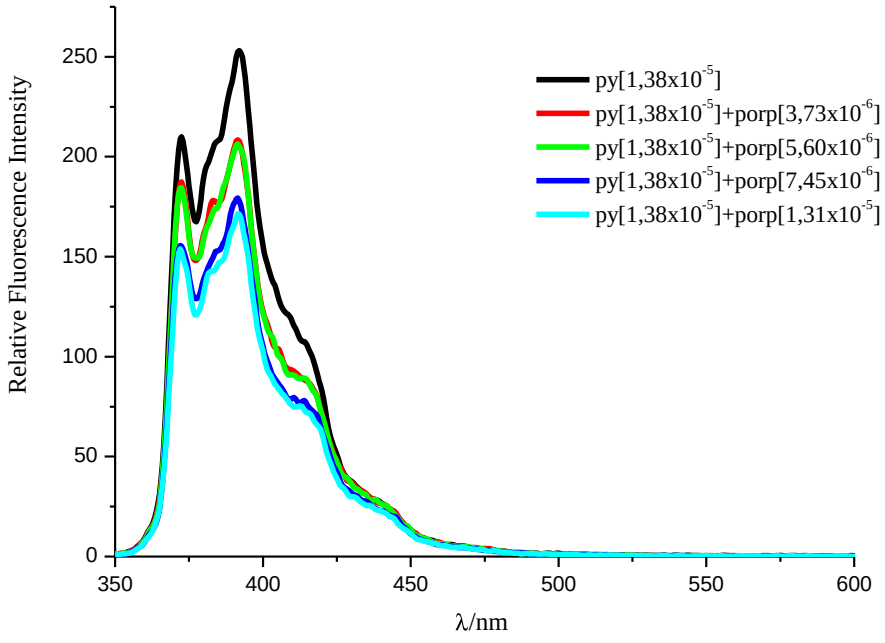

Figure 4.4 Fluorescence spectra of pyrene-protoporphyrin system in DCM

The fluorescence spectra of **py-protoporp** system are seen from Figure 4.4. Pyrene has three characteristic vibration bands at nearly 371, 391 and 415 nm in

DCM. The 0-0 transition has been proved at 371 nm. When the concentration of **protoporp** is increased, there is significant quenching at vibration bands of **py**. The quenching of pyrene monomer fluorescence is explained that there is an interaction with protoporphyrin in the excited state but there is no new band recorded at long wavelength. Nevertheless it is regarded that the new complex which is formed due to this interaction can be explained by the exciplex formation between the **py** and **protoporp**.

In the other solvents (THF and 2Me-THF) the fluorescence measurements have been repeated and the same results have been observed (Figure 4.5 and Figure 4.6).

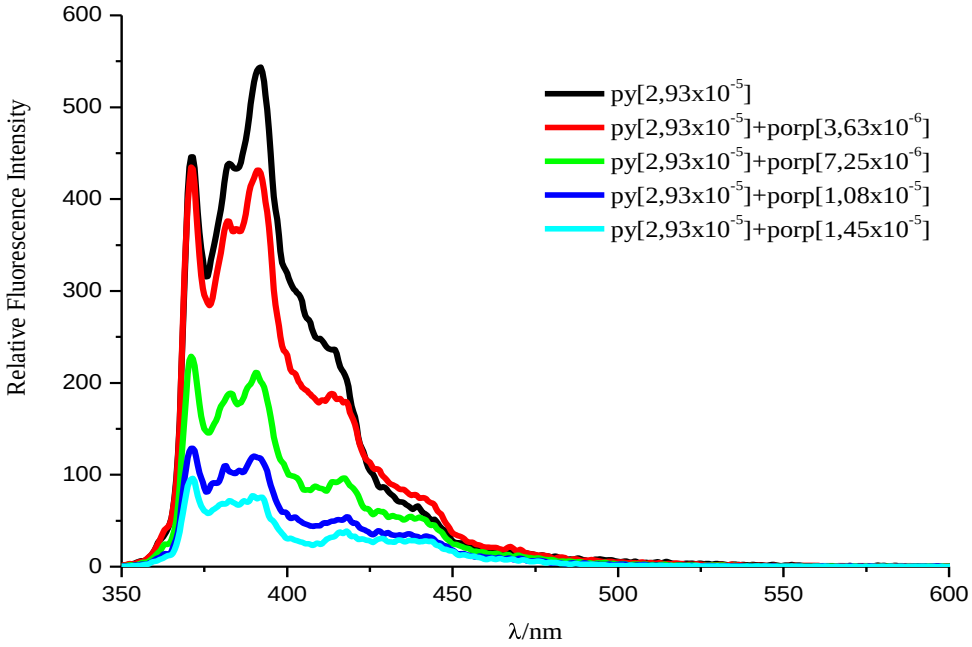

Figure 4.5 Fluorescence spectra of pyrene-protoporphyrin system in THF

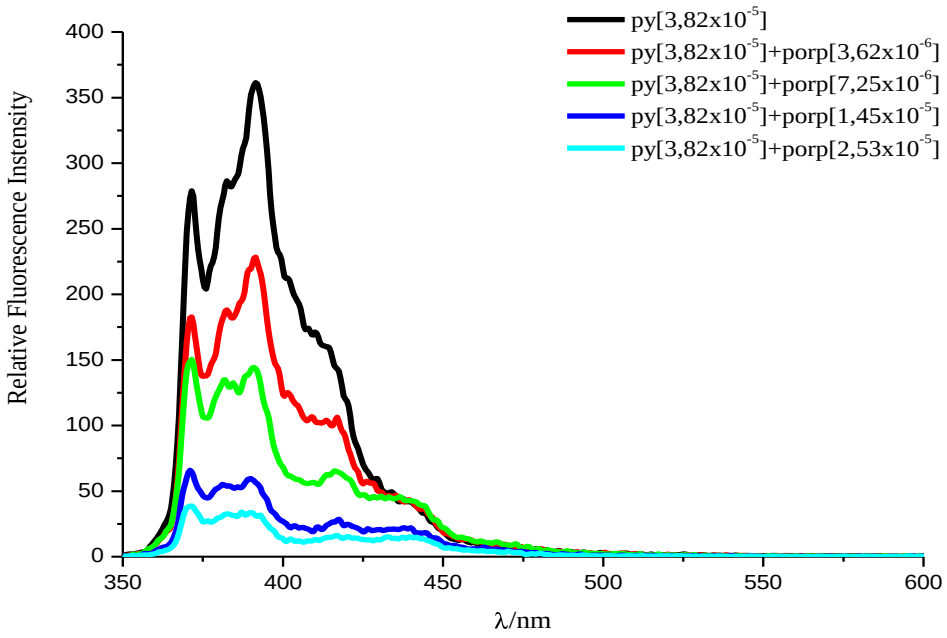

Figure 4.6 Fluorescence spectra of pyrene-protoporphyrin system in 2-Me-THF

4.1.2 Hydroxypyrene-Protoporphyrin(IX) System

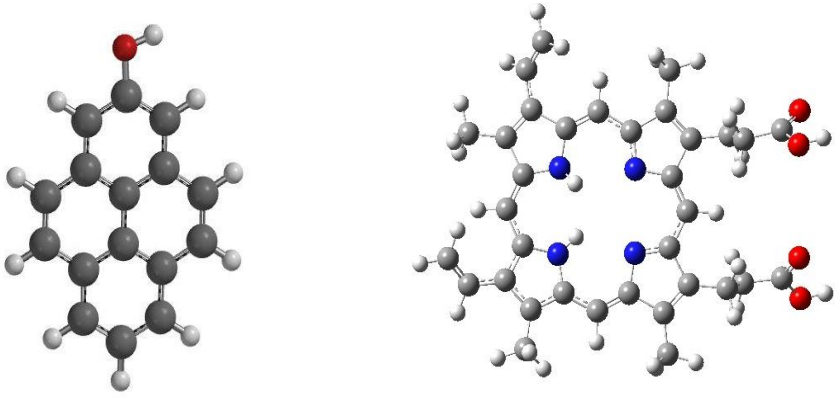

Hydroxypyrene **Protoporphyrin (IX)**

Figure 4.7 Geometric structure of hydroxypyrene and protoporphyrin(IX) with minimum energy calculated by AM1

In hydroxypyrene-protoporphyrin system the concentration of hydroxypyrene is 1.65×10^{-5} M and is fixed during the measurements. The concentration of protoporphyrin is changing between the 1.80×10^{-6} and 1.45×10^{-5} M and all the measurements are repeated. During the measurements, the concentrations of

protoporphyrin are increased and the measurements are repeated. However, the absorption spectra are not changed with adding protoporphyrin. This situation has been shown that there are not any interactions between **pyOH** and **protoporp** in the ground state (Figure 4.9). Nearly 383nm, there is a 0-0 transition which belongs to hydroxypyrene.

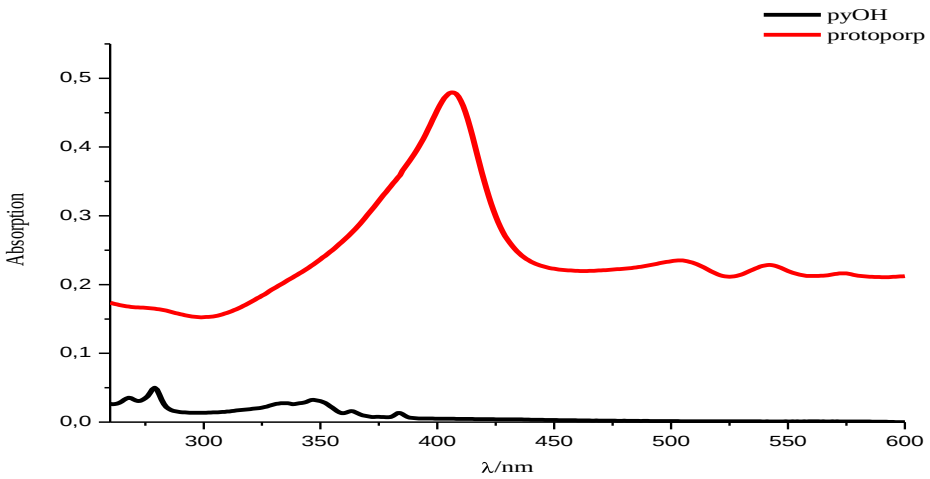

Figure 4.8 UV-Vis spectra of hydroxypyrene and protoporphyrin in DCM

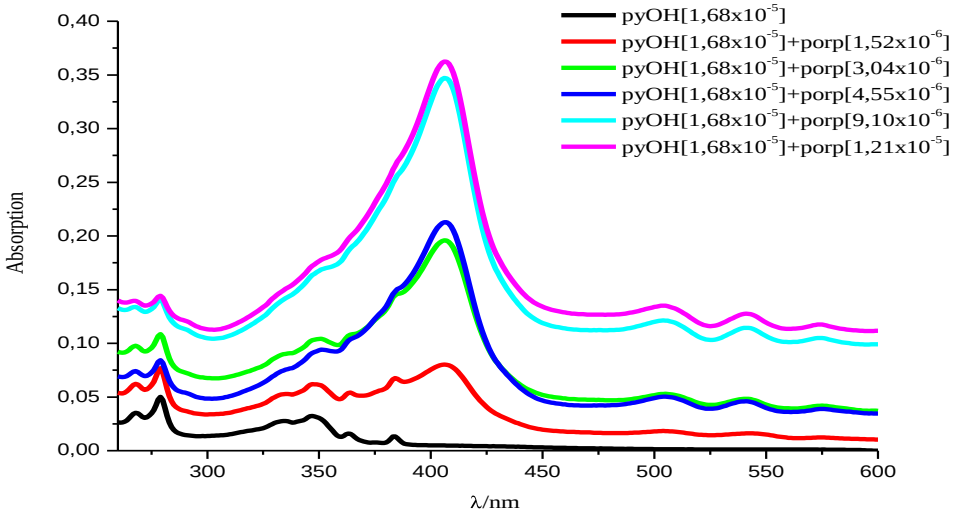

Figure 4.9 UV-Vis spectra of hydroxypyrene-protoporphyrin system in DCM

The fluorescence measurements of hydroxypyrene-protoporphyrin system, have been taken in different solvents (DCM, THF, 2-met-THF). Hydroxypyrene has three characteristic vibration bands at 383(0-0 transition), 403 and 427 nm. In this system the excitation wavelength is chosen at 370 nm. When the fluorescence

spectra investigated, it is observed that the monomer fluorescence of hydroxypyrene is quenched by adding protoporphyrin. This quenching can be supported by the exciplex formation between **pyOH** and **protoporp.**

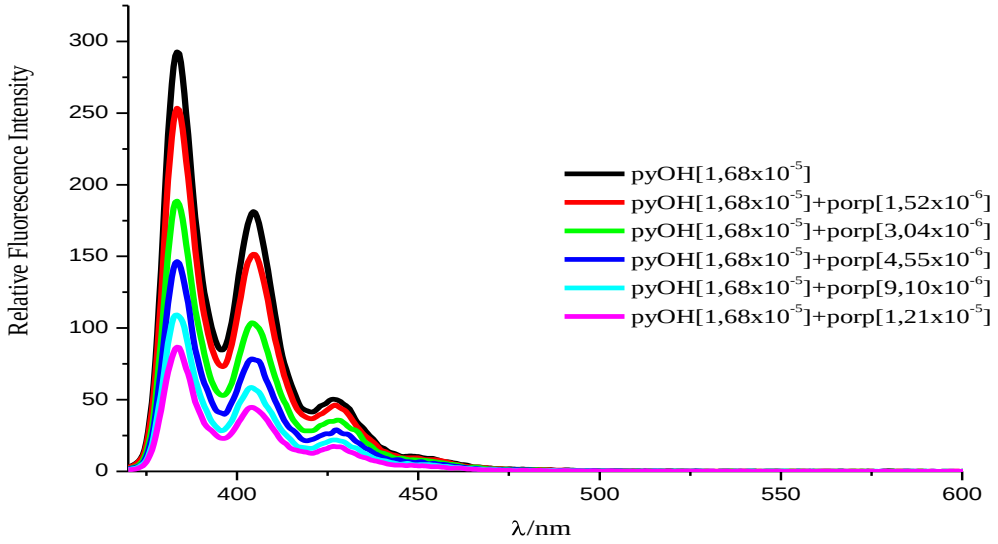

Figure 4.10 Fluorescence spectra of hydroxypyrene-protoporphyrin system in DCM

The fluorescence measurements have been performed again in the other solvents (THF and 2-Me-THF); and the results indicated the same properties (Figure 4.11 and Figure 4.12).

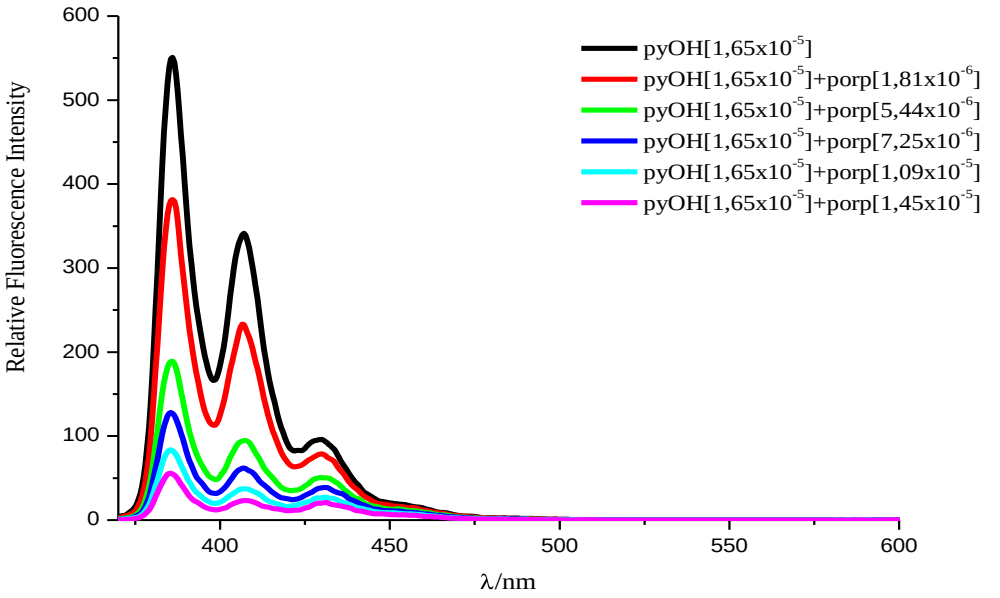

Figure 4.11 Fluorescence spectra of hydroxypyrene-protoporphyrin system in THF

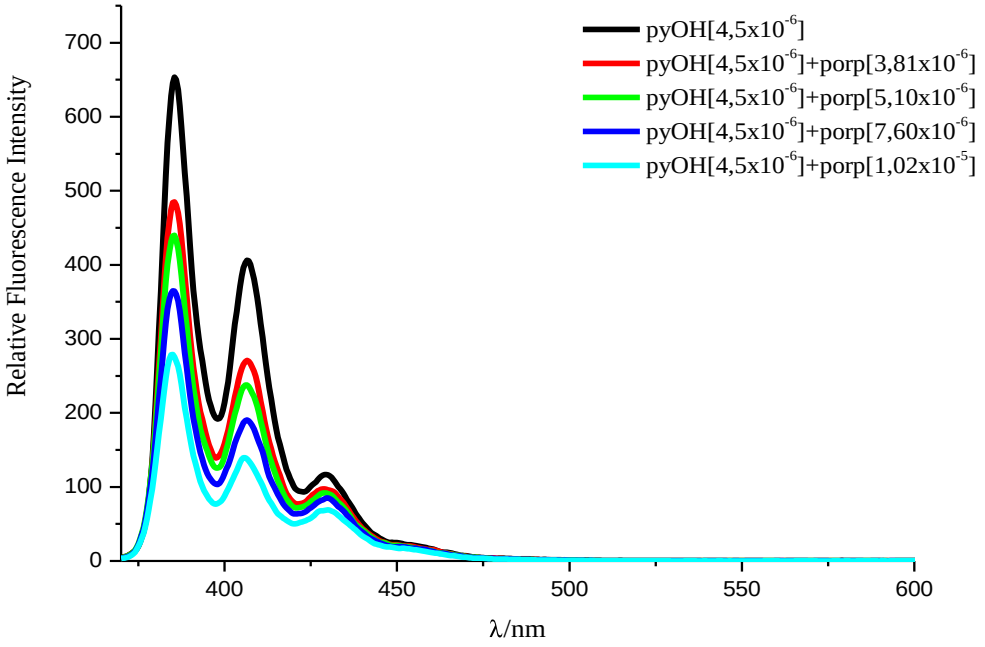

Figure 4.12 Fluorescence spectra of hydroxypyrene-protoporphyrin system in 2-Mel-THF

4.2 Kinetic Investigation

The quenching of the monomer (**py** and **pyOH**) fluorescence intensity is noticeable by forming exciplex. The ratio of the monomer fluorescence intensity with quencher (protoporphyrin) and without quencher is calculated at a certain wavelength. The Stern-Volmer equation obtained from this ratio. If the lifetime of monomer is known, the fluorescence quenching rate constant (k_q) can be found. In this study, fluorescence quenching rate constant (k_q) is calculated by Stern-Volmer equation in different solvents.

$$\frac{I_0}{I} = 1 + k_q . \tau_0 . [Q] \qquad (1.28)$$

In this equation k_q is bimolecular quenching rate constant, I_0 and I are fluorescence intensity of monomer and system respectively, τ_0 is life time without quencher (161 ns and 16.5 for pyrene and hydroxypyrene respectively).(Acar,N. and Kocak, Ö., 2002)

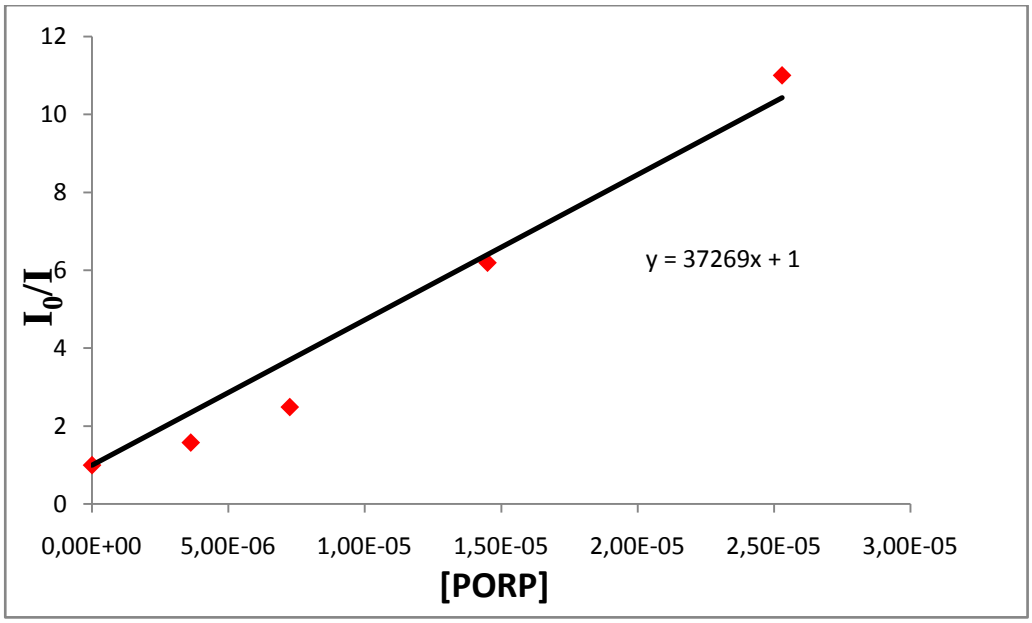

Figure 4.13 The Stern-Volmer graphic of pyrene-protoporphyrin system in 2-Methyl-THF

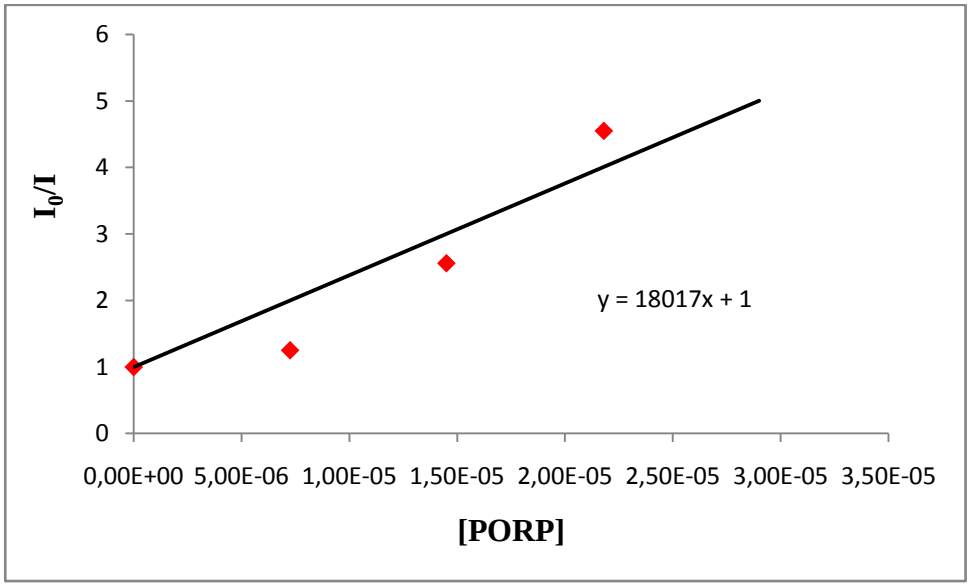

Figure 4.14 The Stern-Volmer graphic of pyrene-protoporphyrin system in THF

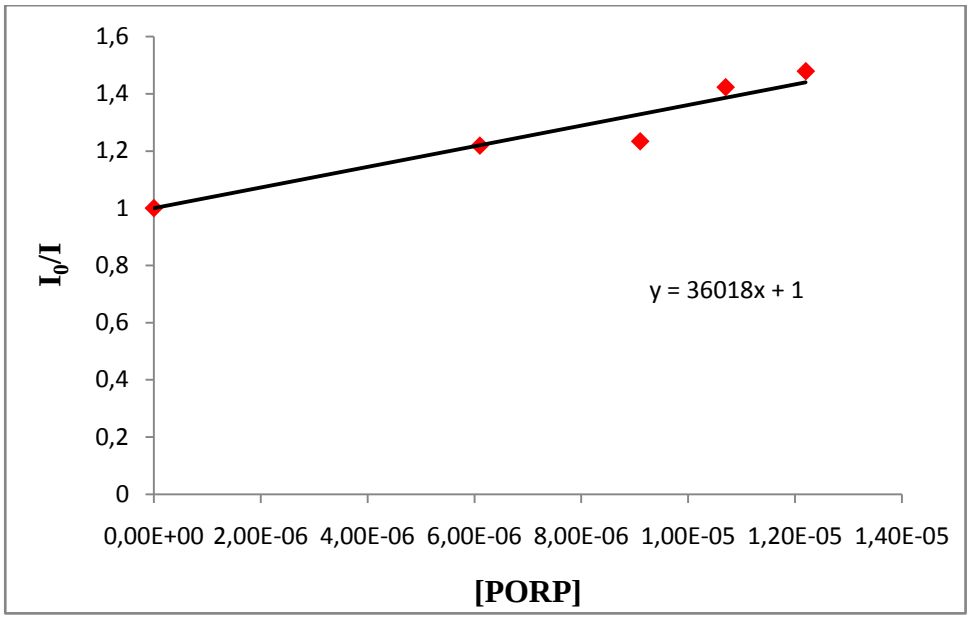

Figure 4.15 The Stern-Volmer graphic of pyrene-protoporphyrin system in DCM

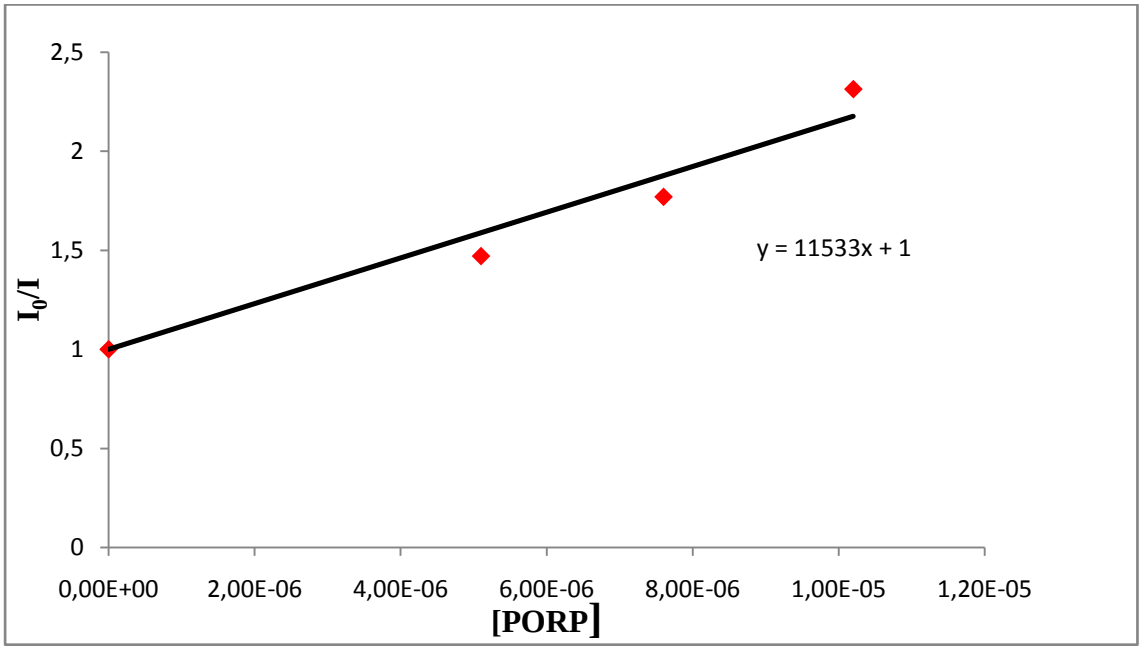

Figure 4.16 The Stern-Volmer graphic of hydroxypyrene-protoporphyrin system in 2-methyl THF

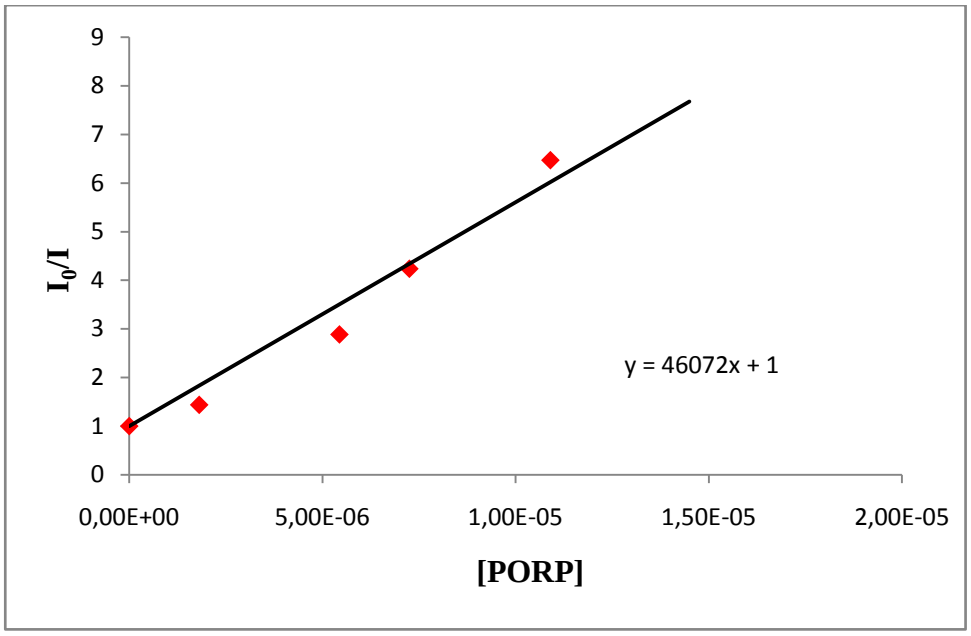

Figure 4.17 The Stern-Volmer graphic of hydroxypyrene-protoporphyrin system in THF

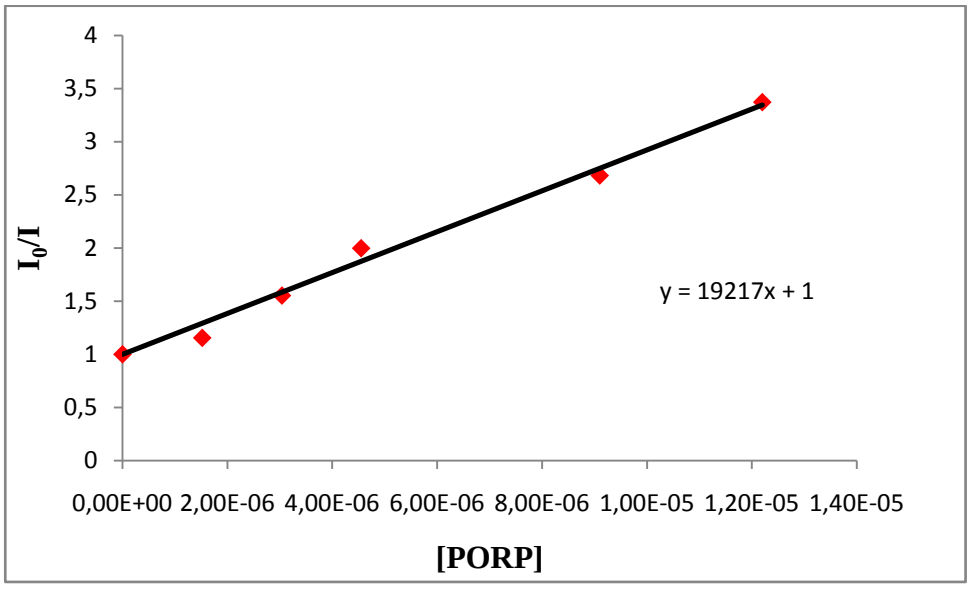

Figure 4.18 The Stern-Volmer graphic of hydroxypyrene-protoporphyrin system in DCM

Table 4.1 Quenching rate constants for py-protoporp and pyOH-protoporp systems

Solvents	ε	μ (Debye)	py-porp system	pyOH-porp system
			$k_q/10^{10}$ (M^{-1} s^{-1})	$k_q/10^{11}$ (M^{-1} s^{-1})
2-Met-THF	6.97	1.38	10.86	6,98
THF	7.52	1.75	11.19	27.92
DCM	9.10	1.60	22.37	11.65

In Table 4.1 the fluorescence quenching rate constants of the systems investigated have been seen. The intermolecular complex formation is supported by having high rate constant. Those constants are found in the order of 10^{10} and 10^{11}, that is diffusion controlled quenching rate constant order. Because molecules are affected by environment; as solvent polarity increases, their approach and interaction rate constant decreases.(in DCM for pyrene τ_0=161 ns; in THF and 2-methyl THF for pyrene τ_0=343 ns; in DCM, THF and 2-methyl THF for hydroxypyrene τ_0=16.5 ns)

4.3 Computational investigation

Acceptors, donors and complex molecules are optimized AM1, PM3 and DFT methods in Gaussian 98 and harmonic oscillator vibration frequencies are characterized at this ground state geometry with the same methods.

Electronic and geometric structure of molecules affects their interactions and properties. In order to understand the mechanisms of interaction between the molecules in their ground state geometric and electronic structures must be assigned correctly. So that primarily ground state geometries and electronic energies of donor and acceptor molecules and complexes calculated by semi-empirical AM1 and PM3 methods and DFT-B3LYP/6-31G(d) and PBE1PBE/6-31G(d) methods. Properties of optimized geometries with B3LYP/6-31G(d) and PBE1PBE/6-31G(d) not different and so the optimized geometries of donors and

acceptors calculated by DFT and with PBE1PBE/6-31G(d) have been displayed Figure 4.19, 4.20, 4.21 and 4.22.

For the donor and acceptor molecules and complexes calculated by AM1, PM3 and B3LYP and PBE1PBE methods calculated the absolute zero energies,harmonic vibration frequencies ansd point group symmetries have been displayed in Table 4.2, 4.3, 4.4,4.5, and 4.6.

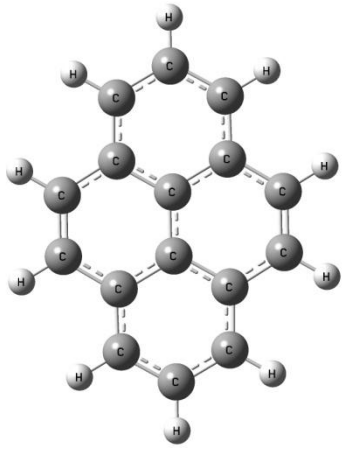	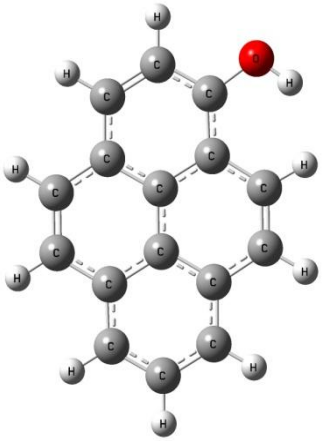
Pyrene	**Hydroxypyrene**

Figure 4.19 The optimized geometries of acceptor molecules calculated with DFT-PBE1PPBE/6-31G(d)

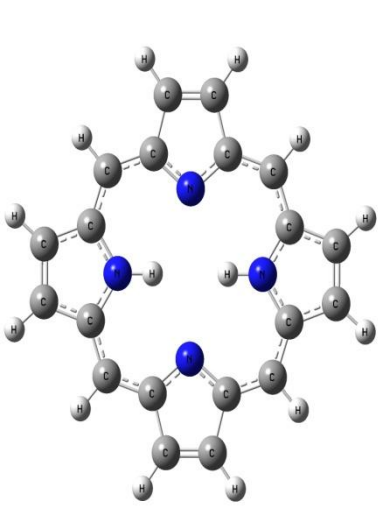

Porphyrin

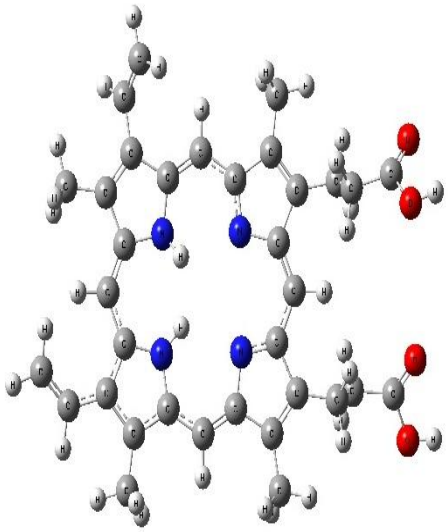

Protoporphyrin IX

Figure 4.20 The optimized geometries of donor molecules (for porphyrin calculated with DFT-PBE1PBE/6-31G(d) ; for protoporphyrin calculated with PM3

Table 4.2 Energies at absolute zero(atomic units),the lowest vibrational energies and point group symmetries of acceptor and donor molecules calculated with PBE1PBE/6-31G(d) method (A=acceptor; D=donor)

Reactant molecules	E_0 (PBE1PBE/631G(d))	The lowest vibrational frequency (cm^{-1})	Point group symmetry
Pyrene(A)	-614.842131	100.4	D_{2h}
1-Hydroxypyrene (A)	-689.980175	65.1	C_s
Porphyrin (D)	-988.119453	55.1	C_{2v}

Table 4.3 Energies at absolute zero(atomic units),the lowest vibrational energies and point group symmetries of acceptor and donor molecules calculated with AM1 and PM3 methods (A=acceptor; D=donor)

Reactant molecules	E_0 (a.u)		The lowest vibrational frequency (cm^{-1})		Point group symmetry	
	AM1	PM3	AM1	PM3	AM1	PM3
Pyrene(A)	0.10691	0.10182	86.57	82.29	D_{2h}	D_{2h}
Hydroxypyrene (A)	0.03758	0.03222	79.76	73.45	C_s	C_s
Porphyrin(D)	0.691425	0.590611	49.10	14.00	D_{2h}	C_s
Protoporphyrin (D)	0.063750	-0.02693	10.51	10.36	C_1	C_1

Table 4.4 Energies at absolute zero(atomic units),the lowest vibrational energies and point group symmetries of acceptor and donor molecules calculated with B3LYP/6-31G(d) method (A=acceptor; D=donor)

Reactant molecules	E_0 (B3LYP/631G(d))	The lowest vibrational frequency(cm^{-1})	Point group symmetry
Pyrene(A)	-615.565435	101.1	D_{2h}
Hydroxypyrene (A)	-690.775918	64.1	C_s
Porphyrin (D)	-989.254878	55.7	C_{2v}

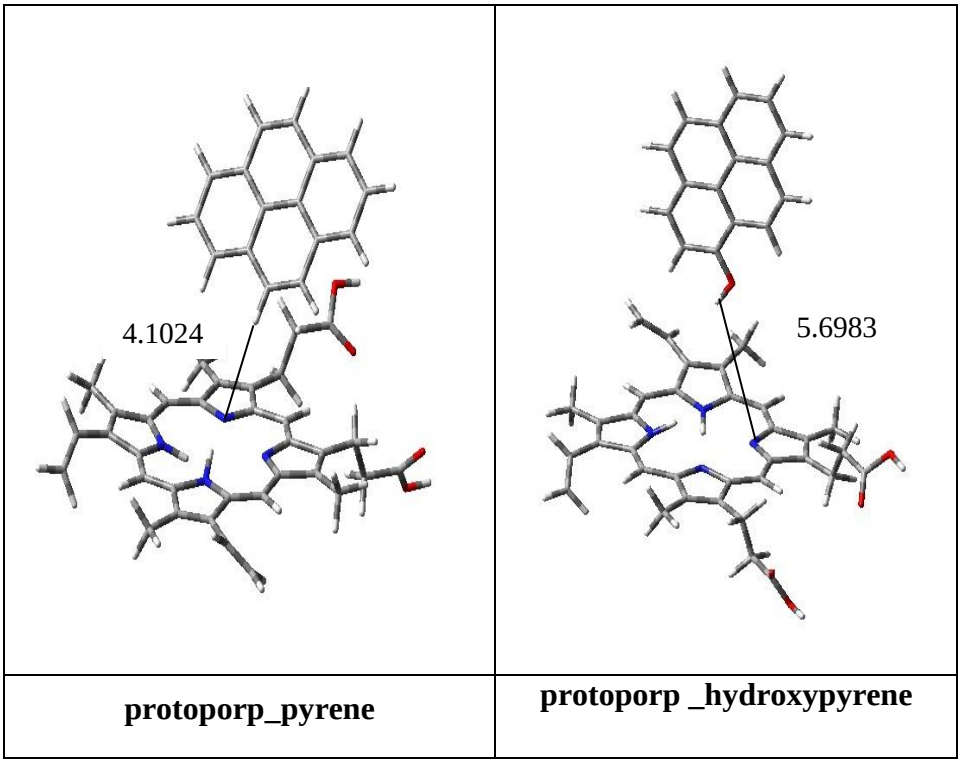

protoporp_pyrene	protoporp _hydroxypyrene

Figure 4.21 The optimized geometries of protoporp_py and protoporp_pyOH calculated complexes with AM1

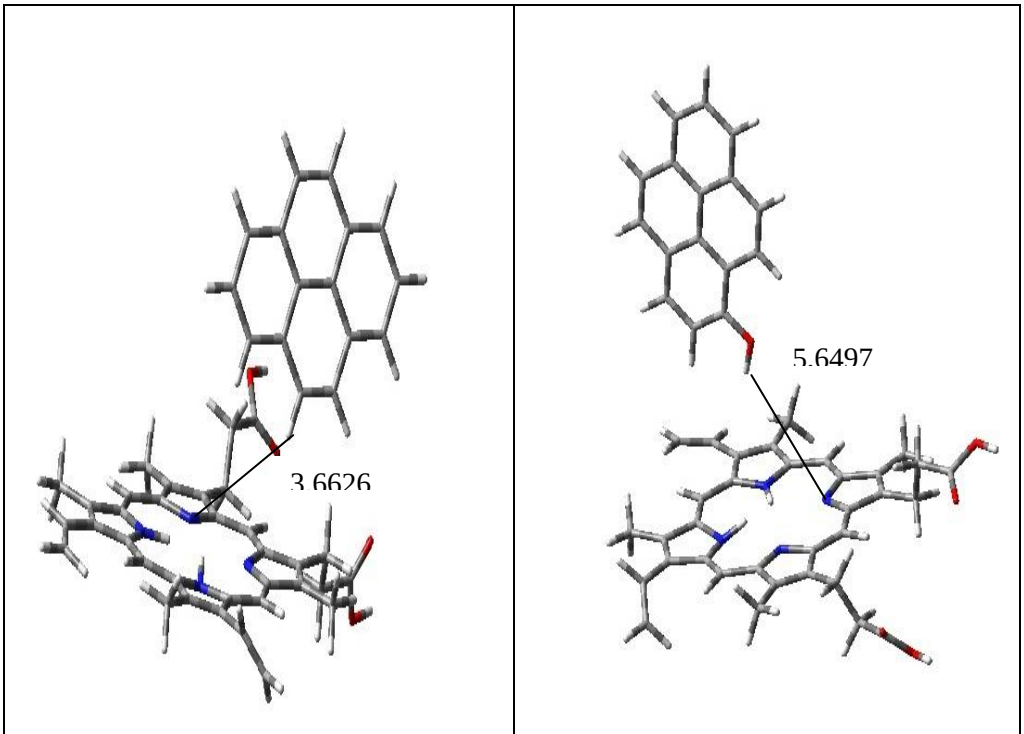

protoporp_pyrene	protoporp _hydroxypyrene

Figure 4.22 The optimized geometries of protoporp_py and proto porp_pyOH complexes calculated with PM3

Table 4.5 Energies at absolute zero(atomic units),the lowest vibrational energies and point group symmetries of complexes calculated with AM1 and PM3

Complex	E_0(a.u)		The lowest vibrational frequency(cm^{-1})		Point group symmetry	
	AM1	PM3	AM1	PM3	AM1	PM3
protoporp_py	0.170604	0.06695	1.9286	3.6855	C_1	C_1
protoporp_pyOH	0.098416	0.00091	2.8705	2.1728	C_1	C_1

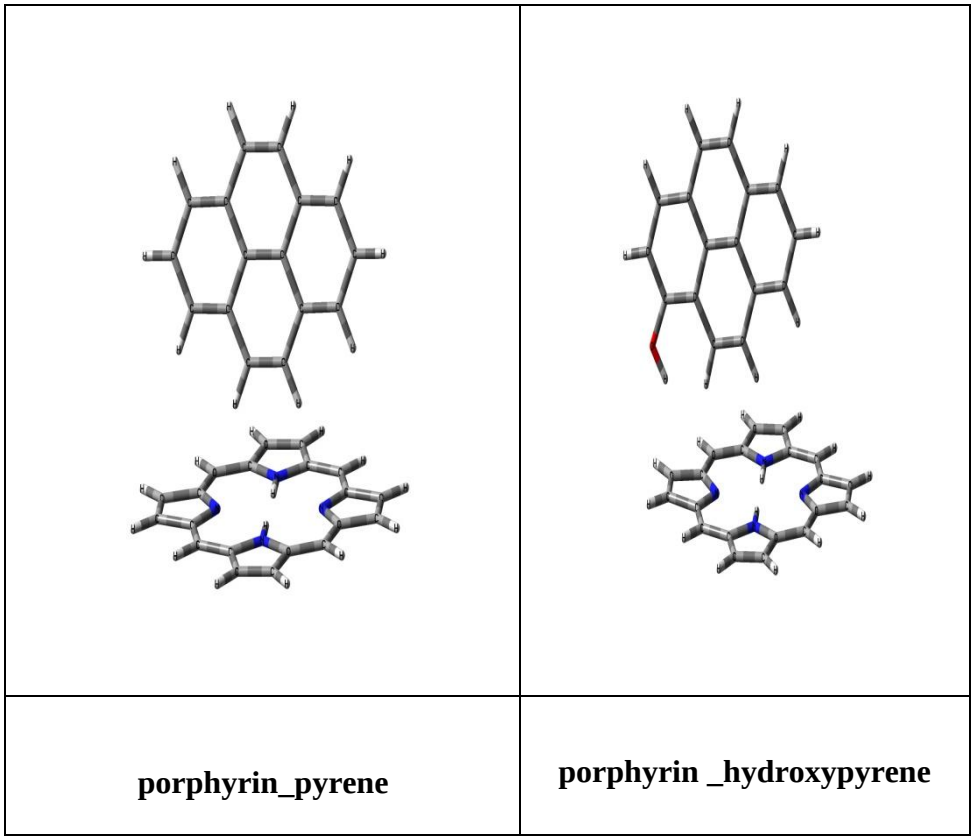

porphyrin_pyrene | **porphyrin _hydroxypyrene**

Figure 4.23 The optimized geometries of porp_py and porp_pyOH complexes calculated with DFT-PBE1PBE/6-31G(d)

Table 4.6 Energies at absolute zero (atomic units),the lowest vibrational energies and point group symmetry of complexes calculated by DFT-PBE1PBE/6-31G(d)

Complex	E_0 (a.u)	The lowest vibrational frequency(cm^{-1})	Point group symmetry
porp_py	-1602.967024	6.5	C_1
porp_pyOH	-1678.108167	6.8	C_1

Table 4.7 The thermodynamic properties (the energy at infinite zero; E_0, the enthalpy at 298 K; H_{298}, free energy change at 298 K; G_{298}) of porphyrin complexes calculated by DFT-PBE1PBE

Molecule	E_0 (a.u)	H_{298} (Hartree)	G_{298}(Hartree)
porp_py	-1780.979267	-1780.947973	-1603.033166
porp_pyOH	-1678.108167	-1678.077629	-1678.169926

Table 4.8The thermodynamic parameters (the energy of reaction at infinite zero; ΔE_0 (kcal/mol), the enthalpy change 298 K ΔH_{298} (kcal/mol); free energy change at 298 K; ΔG_{298} (kcal/mol); entropy change ΔS; kcal/mol K) of reactions calculated by DFT-PBE1PBE/6-31G(d)

Reaction	ΔE_0	ΔH^0	ΔG^0	ΔS^0
$porp_{(g)} + py_{(g)} \rightarrow porp\_py_{(g)}$	-3.41	-2.41	3.61	-0.0202
$porp_{(g)} + pyOH_{(g)} \rightarrow porp\_pyOH_{(g)}$	-5.36	-5.19	6.42	-0.0389

Table 4.9 The thermodynamic parameters (the energy of reaction at infinite zero; ΔE_0 (kcal/mol), the enthalpy change 298 K ΔH_{298} (kcal/mol); free energy change at 298 K; ΔG_{298} (kcal/mol); entropy change ΔS; kcal/mol K)of reactions calculated by PM3

Reaction	ΔE_0	ΔH^0	ΔG^0	ΔS^0

$protoporp_{(g)} + py_{(g)} \rightarrow protoporp\_py_{(g)}$	-4.78	-3.90	4.91	-0.0295
$protoporp_{(g)} + pyOH_{(g)} \rightarrow protoporp\_pyOH$	-2.58	-1.67	5.97	-0.0256

The thermodynamic properties of complexes (porp_py and porp_pyOH) and complex reactions between porphyrin (donor) and pyrene, hydroxypyrene (acceptors) can be seen from Table 4.8 and 4.9.

Table 4.10 HOMO-LUMO energies and dipole moment, μ (Debye), values of acceptor and donor molecules obtained with B3LYP/6-31G(d) and for protoporphyrin obtained with PM3(A=acceptor; D=donor)

Reactant molecules	E_{HOMO} (eV)	E_{LUMO} (eV)	μ (D)
Pyrene(A)	-5.33	-1.47	0.0
Hydroxypyrene(A)	-5.10	-1.42	1.0
Porphyrin(D)	-5.15	-2.24	0.0
Protoporphyrin(D)	-8.35	-1.75	3.1

HOMO-LUMO energies and dipole moment values of acceptor and donor molecules obtained with B3LYP/6-31G(d) have been displayed in Table 4.10.

Table.4.11 The difference between LUMO energies of acceptor molecules and HOMO energies of donor molecules

Donor/acceptor	ΔE_{LUMO_HOMO} (kcal/mol)

	Py	pyOH
Porphyrin	115.70	117.30
Protoporphyrin	158.66	159.81

The two molecules reactivity mainly is determined according to the molecules are charged and the energy of the boundary molecular orbital.

This interaction is given by the Klopman equation (equation 4.1):

$$\Delta E = -\frac{Q_D Q_A}{\varepsilon R} + 2\sum_n \sum_m \frac{\left(c_m^D c_n^A \beta\right)^2}{(E_m - E_n)} \qquad (4.1)$$

In this equation;

Q: Charge density,

ε: Dielectric constant,

R: The distance between donor and acceptor atoms,

c: The number of molecular orbital,

n: The n. occupied molecular orbital of donor molecule,

m: The m. unoccupied molecular orbital of acceptor molecule,

β: Overlap integral,

E: The energy of molecular orbital (Klopman, 1968).

The first term in this equation is determined as charge/charge interaction and its value depends on the molecules charges, Coulomb interaction which depends on the distance between them and the decomposer's polarity. For instance, the differently charged molecules (+/-) are more reactive than the same charged molecules. The second term in the Klopman equation is $HOMO_D/LUMO_A$ interaction ($HOMO_D$: donor HOMO, $LUMO_A$: acceptor LUMO) and the value is mainly determined by the energy diversity between the full molecular orbital on the donor and the empty molecular orbital on the acceptor. If the energy diversity between the frontier orbital is decreased, the interaction between molecules is increased, depending on this donor-acceptor complex creating affinity of molecules is increased.

Table 4.12 $S_0 \rightarrow S_1$ transitions of porp and protoporp donor-acceptor complex molecules (CT=charge transer LE=local excitation)

Complex	E_{exc} (eV)	λ_{exc} (nm)	Oscillator strength (f)	Transitions	Transition character
Porp_py	2.24	554	0.0001	$H \rightarrow L$	CT
Porp_pyOH	1.83	676	0.0030	$H \rightarrow L$	CT
Protoporp_py	2.22	558	0.0861	$H \rightarrow L$	LE
Protoporp_pyOH	2.03	610	0.0000	$H \rightarrow L$	CT

$S_0 \rightarrow S_1$ vertical electronic excitation energies, excitation wavelength, the spectroscopic transitions and their characters are given in the Table 4.12. The character of an electronic transition is determined by analyzing the MOs of donor-acceptor complex obtained from TD-DFT calculations. If the transition occurs from one of the occupied frontier occupied MO of donor molecule to one of the vacant MO of acceptor molecule, this transition is called charge transfer (CT) transition. Conversely, if the transition occurs among frontier MOs either donor or acceptor molecule, this transition is called local excitation (LE). Kohn-Sham molecular orbitals for complexes are given in the Figure 4.24.

Complex	$\lambda_{(exc)}$ (nm)	Transitions		
Porp_py	554	HOMO 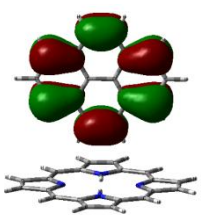	→	LUMO 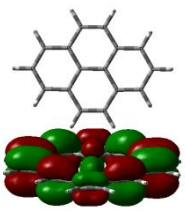

Porp_pyOH	676	HOMO 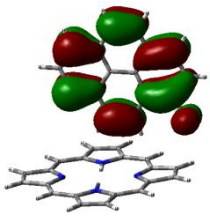	→	LUMO 
Proto_py	558	HOMO 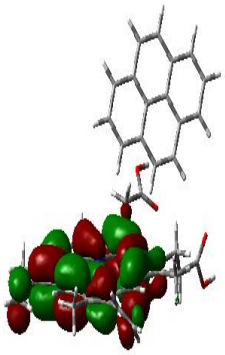	→	LUMO 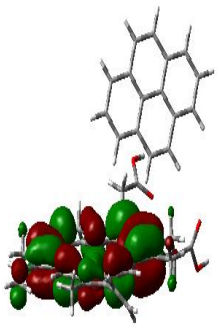
Proto_pyOH	610	HOMO 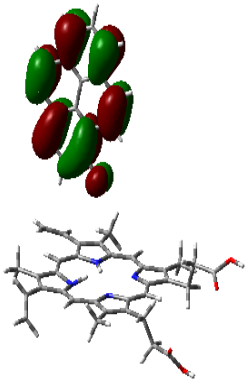	→	LUMO 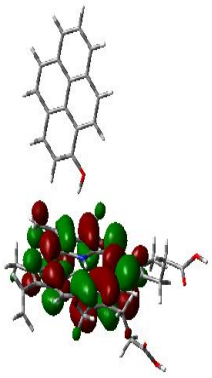

Figure 4.24 $S_0 \rightarrow S_1$ electronic transitions of porphyrin and protoporphyrin complex molecules and Kohn-Sham molecular orbitals of these transitions obtained with TD-B3LYP/6-31G(d)

5. CONCLUSION

The investigations have been performed with the solvents in which protoporphyrin can dissolve. Although the donor-acceptor systems were studied in medium-polarity solvents, there were some differences in k_q values. These quenching rate constants were found to be diffusion controlled by using Stern-Volmer equation. The solvent polarity increases in the order 2-methyl tetrahydrofuran, tetrahydrofuran and dichloromethane. The k_q values decreases

with increasing solvent polarity. The largest value for pyrene-protoporphyrin system was observed in 2-methyl tetrahydrofuran. This observation may show that molecules approach each other faster in low-polarity solvents and van der Waals interactions may form.

The k_q values for hydroxypyrene-protoporphyrin system are larger than that of pyrene-protoporphyrin system. This can be explained by the effect of OH group in hydroxypyrene.

Minimum energy geometries and their electronic structures for separate molecules and for the complexes they form have been obtained by using DFT-PBE1PBE/6-31G(d) and PM3 methods. These calculations indicate that van der Waals interactions are present between donor and acceptor molecules in the gas phase so they form stable complexes in the ground state at absolute zero. On the other hand, the complex formation is thermodynamically unfavorable due to the entropic effect at elevated temperatures e.g. room temp (25°C). Furthermore, the DFT-PBE1PBE/6-31G(d) level calculations indicated that porphyrin-hydroxypyrene system has a lower energy than the pyrene system. As a result the former system is more stable.

In order to explain the singlet electronic transitions, complex transitions have been investigated. The results indicated that HOMO-LUMO energy gaps of porphyrin complexes (115.70 and 117.30 kcal/mol) and protoporphyrin complexes (158.66 and 159.81kcal/mol) are similar.

All the electronic transitions and transition characteristics of complexes have been determined by using TD-DFTB3LYP method. Among these, CT character was observed between py_porp complex, pyOH_porp and pyOH_protoporp complex. HOMO-LUMO transition in py_protoporp indicates that porphyrin parts belong to LE above 558 nm. This observation is in agreement with the experimental result showing an absorption peak for porphyrin at 550 nm. CT transition calculated between pyrene-porphyrin and hydroxypyrene-protoporphyrin cannot be observed experimentally. The oscillator strengths of

complexes respectively 0.0001 and 0.0000 obtained by computational methods indicate that these peaks are either unobservable or very weak.

REFERENCES

Acar, N., Koçak, Ö., 2002, Thermodynamic and Kinetic Parameters Concerning Complex Formation between 3-Hydroxy and 1-Aminopyrene and Pyridine, Turkish Journal Chem., 26,2,201p.

Bauernschmitt, R., Ahlrichs, R., 1996, Calculation of excitation energies within time-dependent density functional theory using auxiliary basis set expansions, Chemical Physics Letters, 256:454p.

Birks, J. B., Alwattar, A. J. H., Lumb, M. D., 1971, The influence of the solvent viscosity on the radiative and radiationless transition rates of the pyrene excimer, Chemical Physics Letters, 11(1):89-92pp.

Birks, J. B., Lumb, M. D., and Munro, I. H., 1964, Temperature studies of the fluorescence pyrene solutions, Acta Physica Polonica, 26 (3-4):379-386pp.

Böttcher C.J.F., 1973 "Theory of Electric Polarization", Elsevier, Amsterdam.

Casida, M. E., 1995, in: d.P. Chong (Ed.), Recent Advances in Density Functional Methods, Band I, World Scientific, Singapore.

Coulson C.A., O'Leary B., Mallion R.B., 1978, Hückel Theory for Organic

Chemists, and Academic Press.

Fetzer, J. C., 2000 , "The Chemistry and Analysis of the Large Polycyclic Aromatic Hydrocarbons". *Polycyclic Aromatic Compounds* (New York: Wiley) **27**: 143.

Förster, T., and Kasper, K., 1955, Ein konzentrationsumschlag der fluoreszenz des pyrens, Zeitschrift für Physikalische Chemie, Neue Folge 59(10): 976-980pp.

REFERENCES (continue)

Frisch, M. J., Trucks, G. W., Schlegel, H. B., Scuseria, G.E., Robb, M. A., Cheeseman, J. R., Zakrzewski, V.G., Montgomery, J. A., Stratmann, Jr., Burant, R. E., Dapprich, J.C., Millam, J. M., Daniels, A. D., Kudin, K. N., Strain, M. C., Farkas, O., Tomasi, J., Barone, V., Cossi, M., Cammi, R., Mennucci, B., Pomelli, C., Adamo, C., Clifforf, S., Ochterski, J., Peterson, G. A., Ayala, P. Y., Cui, Q., Morokuma, K., Salvador, P., Dannenberg, J.J., Malick, D. K., Rabuck, A. D., Raghavachari, K., Foresman, J. B., Cioslowski,

J., Ortiz, J. V., Baboul, A. G., Stefanov, B.B., Liu, G., Liashenko, A., Piskorz, P., Komaromi, I., Gomperts, R., Martin, R. L., Fox, D. J., Keith, T., Al-Laham, M. A., Peng, C. Y., Nanayakkara, A., Challacombe, M., Gill, P. M. W., Johnson, B., Chen, W., Wong, M. W., Andres, J. L., Gonzalez, C., Head-Gordon, M., Replogle, E. S. And Pople, J. A., 2002, Gaussian, Inc. Pittsburgh PA, Gaussian 98,Revision A.11.4.

Furche, F., 2001, On the density matrix based approach to time-dependent density functional response theory, Journal of Chemical Physics, 114:5982p.

Gilbert, A., and Baggott , N., 1991, Essentials of Molecular Photochemistry(London: Blackwell)

Gispert, J.R., 2008, Coordination Chemistry. Wiley-VCH. 483. p.

Görling, A., Heinze, H. H., Ruzankin, S. Ph., Staufer, M. und Rösch, N., 1999, Density and density- matrix-based coupled Kohn-Sham methods for dynamic polarizabilities and excitation energies of molecules, Journal of Chemical Physics, 110:2785p.

Gross, E. K. U., Dobson, J. F., M. Petersilka, 1996, R.F.Nalewajski (Ed.), Density Functional Theory II, Springer Series in Topics in Current Chemistry, Springer, Heidelberg, 181:81p.

Hoffmann R., 1963, Journal of Chemical Physics, 39, 1397.

REFERENCES (continue)

Hohenberg, P., Kohn W., 1964, Inhomogeneous Electron Gas, Physical Review, 36, B864.

Hückel E., Zeitschrift für Physik, 70, 204, (1931); 72, 310, (1931); 76, 628 (1932); 83, 632, (1933).

Jablonski, A., 1935, Über den Mechanism des Photolumineszenz von Farbstoffphosphoren, Z. Phys. 94:38-46

Kavarnos, G. J., 1993, Fundamentals of Photoinduced Electron Transfer, VCH Publisher, New York,359p.

Khalil, M. N. H., Boens, N., and De Schryver, F. C., 1993, Global compartmental analysis of the fluorescence decay surfaces of the exciplex of 1-cyanopyrene and of the exciplex of 1-cyanopyrene with 1,2-dimethylindole in toluene, The Journal of Physical Chemistry, 97, 3111-3122pp.

Kitai, A., 2008, Luminescent Materials and Applications.,John Wiley and Sons. 32. p.

Klopman G., 1968, "Chemical reactivity and the concept of charge and Frontier-contorelled Reactions" , J. Am. Chem Soc, 90:2, 223-234

Kohn, W., Sham, L. J., 1965, Self-Consistent Equation Including Exchange and Correlation Effects, Physical Review, 140:A1133.

Lakowicz, J.R., 1999, Principles of Fluorescence Chemistry, Plenum Press, New York and London,510p.

Levine I.N., 1991, Quantum Chemistry, Printice-Hall,New Jersey.

REFERENCES (continue)

Mataga, N., Kaifu, Y., and Kouzumi, M., 1956, Hydrogen-bonding effect on the fluorescence of p- electron systems, Bulletin of The Chemical Society of Japan, 29(1):115-122pp.

Murrell J.N., "The Theory of the Electronic Spectra of Organic Molecules" , Wiley, New York, 1963.

Palmans, J. P., Van der Auweraer, M., Swinen, A., and De Schryver, F. C., 1984, Intermolecular exciplex formation between Pyrene derivatives and 1-2-Dimethylindole, Journal of American Chemical Society, 106(25):7721-7728pp.

Perdew, J. P., Burke, K., Ernzerhof, M., 1996, Generalized gradient approximation made simple, Physical Review Letters, 77:3865p.

Shinoda S., 2007 , Nanoscale substrate recognition by porphyrin dendrimers with patched structures. J Incl Phenom Macrocycl Chem 59:1-9.

Streitwieser A., 1961, Molecular Orbital Theory for Organic Chemists, Wiley, New York.

Suppan P., 1990, J.Photochem. Photobiol., A50, 293.

Taylor , 2006, Handbook of Photochemistry,Third Edition, Taylor & Francis Group, LLC.

Wardle B., 2009, "Principles and Applications of Photochemistry", Manchester Metropolitan University, Manchester, UK, John Wiley & Sons, Ltd.

Weller , A., 1961, Fast reactions of excited molecules, 189-214 Progress in Reaction Kinetics I, Porter, G.(Ed), Pergamon Press, New York, Oxford, London, Paris, 276p.

. **Wiley J.,** 2007, Introduction to Computational Chemistry, Second Edition, Frank Jensen, John Wiley & Sons, Ltd.

REFERENCES (continue)

Zhao, Y., Truhlar, D. G., 2005, Benchmark Databases for Nonbonded Interactions and Their Use to Test Density Functional Theory, Journal of Chemical Theory and Computation,(1):415p.

CURRICULUM VITAE

Name Surname : Zeliha Gamze Alp

Profession : Chemist

Date/Place of Birth: 1987/Kdz.Eregli

Nationality: Turkish

Gender: Female

Marital Statue: Single

Adress: Ege University, Faculty of Science; Department of Chemistry,

Division of Physical Chemistry, 35100

35100, Bornova-İzmir/Turkey

e-mail: zelihagamze@gmail.com

EDUCATIONAL BACKGROUND:

B.S In Chemistry, 2009, Balikesir University, Balikesir-Turkey